mathematics

MDPI

Article

Modeling and Stability Analysis of Within-Host IAV/SARS-CoV-2 Coinfection with Antibody Immunity

Ahmed M. Elaiw *, Raghad S. Alsulami and Aatef D. Hobiny

Department of Mathematics, Faculty of Science, King Abdulaziz University, P. O. Box 80203, Jeddah 21589, Saudi Arabia

* Correspondence: a_m_elaiw@yahoo.com

Abstract: Studies have reported several cases with respiratory viruses coinfection in hospitalized patients. Influenza A virus (IAV) mimics the Severe Acute Respiratory Syndrome Coronavirus 2 (SARS-CoV-2) with respect to seasonal occurrence, transmission routes, clinical manifestations and related immune responses. The present paper aimed to develop and investigate a mathematical model to study the dynamics of IAV/SARS-CoV-2 coinfection within the host. The influence of SARS-CoV-2-specific and IAV-specific antibody immunities is incorporated. The model simulates the interaction between seven compartments, uninfected epithelial cells, SARS-CoV-2-infected cells, IAV-infected cells, free SARS-CoV-2 particles, free IAV particles, SARS-CoV-2-specific antibodies and IAV-specific antibodies. The regrowth and death of the uninfected epithelial cells are considered. We study the basic qualitative properties of the model, calculate all equilibria and investigate the global stability of all equilibria. The global stability of equilibria is established using the Lyapunov method. We perform numerical simulations and demonstrate that they are in good agreement with the theoretical results. The importance of including the antibody immunity into the coinfection dynamics model is discussed. We have found that without modeling the antibody immunity, the case of IAV and SARS-CoV-2 coexistence is not observed. Finally, we discuss the influence of IAV infection on the dynamics of SARS-CoV-2 single-infection and vice versa.

Keywords: COVID-19; SARS-CoV-2; influenza A virus; coinfection; global stability; Lyapunov function

MSC: 34D20; 34D23; 37N25; 92B05

Citation: Elaiw, A.M.; Alsulami, R.S.; Hobiny, A.D. Modeling and Stability Analysis of Within-Host IAV/SARS-CoV-2 Coinfection with Antibody Immunity. *Mathematics* **2022**, *10*, 4382. https://doi.org/10.3390/math10224382

Academic Editor: Ricardo Lopez-Ruiz

Received: 2 October 2022
Accepted: 16 November 2022
Published: 21 November 2022

1. Introduction

Coronavirus disease 2019 (COVID-19) was detected in December 2019, in Wuhan, China during the season when influenza was still circulating [1]. COVID-19 is caused by a dangerous type of virus called severe acute respiratory syndrome coronavirus 2 (SARS-CoV-2). According to the update provided by the World Health Organization (WHO) on 21 August 2022 [2], over 593 million confirmed cases and over 6.4 million deaths have been reported globally. SARS-CoV-2 is transmitted to people when they are exposed to respiratory fluids carrying infectious viral particles. The implementation of preventive measures such as physical and social distancing, using face masks, hand washing, disinfection of surfaces and getting vaccinated can reduce SARS-CoV-2 transmission. Eleven vaccines for COVID-19 have been approved by WHO for emergency use. These include Novavax, CanSino, Bharat Biotech, Pfizer/BioNTech, Moderna, Serum Institute of India (Novavax formulation), Janssen (Johnson & Johnson), Oxford/AstraZeneca, Serum Institute of India (Oxford/AstraZeneca formulation), Sinopharm and Sinovac [3]. SARS-CoV-2 is a single-stranded positive-sense RNA virus that infects the epithelial cells. SARS-CoV-2 can cause an acute respiratory distress syndrome (ARDS), which has high mortality rates, particularly in patients with immunosenescence [4]. Immunosenescence renders vaccination less effective and increases the susceptibility to viral infections [5].

Influenza viruses are members of the family of Orthomyxoviridae, which are negativesense RNA viruses. There are four distinct influenza viruses, A, B, C and D. Influenza A virus (IAV) can infect a wide range of species. IAV is a significant public health threat, resulting in 15-65 million infections and over 200,000 hospitalizations every year during seasonal epidemics in the United States [6]. IAV infects the uninfected epithelial cells of the host respiratory tract [7]. Both SARS-CoV-2 and IAV have analogous transmission ways, moreover, they have common clinical manifestations including dyspnea, cough, fever, headache, rhinitis, myalgia and sore throat [1]. Viral shedding usually takes place 5 to 10 days in influenza, whereas it does 2 to 5 weeks in COVID-19 [1]. Acute respiratory distress is less common in influenza than COVID-19 [1]. Deaths in influenza cases are less than 1%, while in cases of COVID-19 it ranges from 3% to 4% [1].

It was reported in [8] that 94.2% of individuals with COVID-19 were also coinfected with several other microorganisms, such as fungi, bacteria and viruses. Important viral copathogens include the respiratory syncytial virus (RSV), human enterovirus (HEV), human rhinovirus (HRV), influenza A virus (IAV), influenza B virus (IBV), human metapneumovirus (HMPV), parainfluenza virus (PIV), human immunodeficiency virus (HIV), cytomegalovirus (CMV), dengue virus (DENV), Epstein Barr virus (EBV), hepatitis B virus (HBV) and other coronaviruses (COVs), among which the HRV, HEV and IAV are the most common copathogens [9]. Several coinfection cases of COVID-19 and influenza have been reported in [1,8,10–12] (see also the review papers [13–16]). Based on two separate studies presented in [10,11], COVID-19-influenza coinfection did not result in worse clinical outcomes [10]. In addition, this condition reduced the mortality rate among COVID-19-influenza coinfected patients. Coinfection with influenza virus in COVID-19 patients might render them less vulnerable to morbidities associated with COVID-19, and therefore, a better prognosis overall [11]. In [16], it was found that, although patients with IAV and SARS-CoV-2 coinfection did not experience longer hospital stays compared with those with a SARS COV-2 single-infection, they usually presented with more severe clinical conditions.

Viral interference phenomenon can appear in case of infections with multiple competitive respiratory viruses. One virus may be able to suppress the growth of another virus [17–19]. Disease progression and outcome in SARS-CoV-2 infection are highly dependent on the host immune response, particularly in the elderly in whom immunosenescence may predispose to increased risk of coinfection [17].

Over the years, mathematical models have demonstrated their ability to provide useful insight to gain a further understanding of the dynamics and mechanisms of the viruses within a host level. These models may assist in the development of viral therapies and vaccines as well as the selection of appropriate therapeutic and vaccine strategies. Moreover, these models are helpful in determining the sufficient number of factors to analyze the experimental results and explain the biological phenomena [7]. Stability analysis of the model's equilibria can help researchers (i) to expect the qualitative features of the model for a given set of values of the model's parameters, (ii) to establish the conditions that ensure the persistence or deletion of this infection, and (iii) to determine under what conditions the immune system is stimulated against the infection. Mathematical models of within-host IAV single-infection have been developed in several works. Baccam et al. [20] presented the following IAV-single-infection with limited target cells:

$$\begin{cases} \dot{X} = -\overbrace{\beta XP}^{\text{IAV infectious transmission}}, \\ \dot{I} = \overbrace{\beta XP}^{\text{IAV infectious transmission}} - \overbrace{\gamma I}^{\text{natural death}}, \\ \dot{P} = \overbrace{\kappa I}^{\text{IAV production}} - \overbrace{\pi P}^{\text{natural death}}, \end{cases} \tag{1}$$

where $X = X(t)$, $I = I(t)$ and $P = P(t)$ are the concentrations of uninfected epithelial cells, IAV-infected epithelial cells and free IAV particles, at time t, respectively. The model was fitted using real data from six patients infected with influenza [20].

Several works have been devoted to study IAV single-infection dynamics models (see the review papers [21–24]) by including the effect of innate immune response [20,25], adaptive immune response [26,27] and both innate and adaptive immune responses [5,7,28–30]. Handel et al. [31] presented a mathematical model for within-host influenza infection under the effect of neuraminidase inhibitors drugs. The effect of a combination of neuraminidase inhibitors and anti-IAV therapies was addressed in [26]. In [26], the first equation of model (1) was modified by considering the target cell production and death as:

$$\dot{X} = \overbrace{\alpha X(0)}^{\text{epithelial cells production}} - \overbrace{\alpha X}^{\text{natural death}} - \overbrace{\beta XP}^{\text{IAV infectious transmission}}, \tag{2}$$

where $X(0)$ is the initial concentration of the uninfected epithelial cells.

Model (1) was utilized to characterize the dynamics of SARS-CoV-2 within a host in [32]. Li et al. [33] used Equation (2) for the SARS-CoV-2 infection dynamics. A model with target-cell limited and a model with regrowth and death of the uninfected epithelial cells presented, respectively, in [32,33] were extended and modified by including (i) latently infected epithelial cells [32,34–36], (ii) effect of immune response [37–42], (iii) effect of different drug therapies [35,43,44], and (iv) effect of time delay [45].

Recently, several mathematical models have been developed to characterize the coinfection of COVID-19 with other diseases in epidemiology (between-host), such as COVID-19/HIV [46], COVID-19/Dengue [47], COVID-19/Dengue/HIV [48], COVID-19/ZIKV [49], COVID-19/Bacterial [50], COVID-19/Influenza [51] and COVID-19/Tuberculosis [52]. However, modeling of within-host dynamics of COVID-19 with other pathogen coinfection has been investigated in few papers: SARS-CoV-2/HIV [53], SARS-CoV-2/malaria [54] and SARS-CoV-2/Bacteria [55]. Based on the target cell-limited model (1), Pinky and Dobrovolny [18,19] developed a model for the within-host dynamics of two respiratory viruses coinfection. They suggested that several types of respiratory viruses can suppress the SARS-CoV-2 infection.

The model presented in [18,19] describes the competition between two respiratory viruses. However, the impact of the immune response against the two viruses was not modeled. Further, the regeneration and death of the uninfected epithelial cells were neglected. Furthermore, mathematical analysis of the model was not studied. Therefore, the aim of the present paper is to develop a within-host IAV/SARS-CoV-2 coinfection model with immune response. The model is a generalization of the model presented in [18,19] by incorporating (i) the regrowth and death of the uninfected epithelial cells, and (ii) the impact of SARS-CoV-2-specific antibody and IAV-specific antibody. We study the basic qualitative properties of the proposed model, calculate all equilibria and investigate the global stability of the equilibria. We support our theoretical results via numerical simulations. Finally, we discuss the obtained results.

Our proposed model can be useful to describe the within-host dynamics of coinfection with two or more viral strains, or coinfection of SARS-CoV-2 (or IAV) and other respiratory viruses. Moreover, the model may help to predict new treatment regimens for viral coinfections.

2. Model Formulation

In this section, we present an IAV/SARS-CoV-2 coinfection dynamics model. The dynamics of IAV/SARS-CoV-2 coinfection is presented in the diagram Figure 1. Let us consider following assumptions:

A1 The model considers the interactions between seven compartments: uninfected epithelial cells (X), SARS-CoV-2-infected cells (Y), IAV-infected cells (I), free SARS-CoV-2 particles (V), free IAV particles (P), SARS-CoV-2-specific antibodies (Z) and IAV-

specific antibodies (M). Here, X, Y, I, V, P, Z and M represent the concentrations of the seven compartments.

A2 The uninfected epithelial cells are the target for both SARS-CoV-2 and IAV [18,20,32].

A3 The uninfected epithelial cells are regenerated and die at rates λ and αX, respectively [33,40,42,56].

A4 The SARS-CoV-2-specific antibodies proliferate at rate $\sigma_Z VZ$, decay at rate $\mu_Z Z$ and neutralize the SARS-CoV-2 particles at rate $\varkappa_V VZ$ [45,57].

A5 The IAV-specific antibodies proliferate at rate $\sigma_M PM$, decay at rate $\mu_M M$ and neutralize the IAV particles at rate $\varkappa_P PM$ [56].

Based on Assumptions A1–A5, we formulate the IAV/SARS-CoV-2 coinfection dynamics model as:

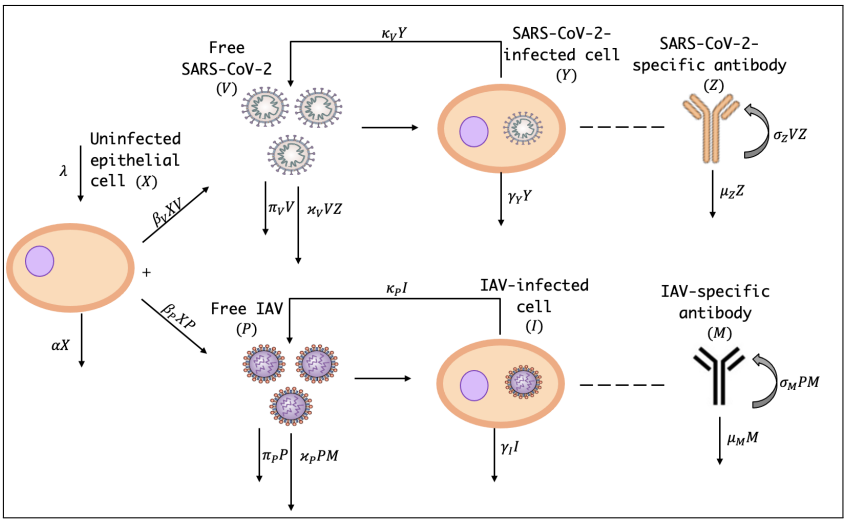

Figure 1. The schematic diagram of the IAV/SARS-CoV-2 coinfection dynamics within-host.

$$\begin{cases} \dot{X} = \overbrace{\lambda}^{\text{epithelial cells production}} - \overbrace{\alpha X}^{\text{natural death}} - \overbrace{\beta_V XV}^{\text{SARS-CoV-2 infectious transmission}} - \overbrace{\beta_P XP}^{\text{IAV infectious transmission}}, \\ \dot{Y} = \underbrace{\overbrace{\beta_V XV}^{\text{SARS-CoV-2 infectious transmission}}}_{\text{IAV infectious transmission}} - \overbrace{\gamma_Y Y}^{\text{natural death}}, \\ \dot{I} = \underbrace{\overbrace{\beta_P XP}^{\text{IAV infectious transmission}}}_{\text{SARS-CoV-2 production}} - \overbrace{\gamma_I I}^{\text{natural death}}, \\ \dot{V} = \underbrace{\overbrace{\kappa_V Y}^{\text{SARS-CoV-2 production}}}_{\text{IAV production}} - \overbrace{\pi_V V}^{\text{natural death}} - \overbrace{\varkappa_V VZ}^{\text{SARS-CoV-2 neutralization}}, \\ \dot{P} = \underbrace{\overbrace{\kappa_P I}^{\text{IAV production}}}_{\text{SARS-CoV-2-specific antibody proliferation}} - \overbrace{\pi_P P}^{\text{natural death}} - \overbrace{\varkappa_P PM}^{\text{IAV neutralization}}, \\ \dot{Z} = \underbrace{\overbrace{\sigma_Z VZ}^{\text{SARS-CoV-2-specific antibody proliferation}}}_{\text{IAV-specific antibody proliferation}} - \overbrace{\mu_Z Z}^{\text{natural death}}, \\ \dot{M} = \overbrace{\sigma_M PM}^{\text{IAV-specific antibody proliferation}} - \overbrace{\mu_M M}^{\text{natural death}}. \end{cases} \tag{3}$$

3. Basic Qualitative Properties

In this section, we study the basic qualitative properties of system (3). We establish the nonnegativity and boundedness of the system's solutions to ensure that our model is biologically acceptable. Particularly, the concentrations of the model's compartments should not become negative or unbounded.

Lemma 1. *The solutions of system (3) are nonnegative and bounded.*

Proof. We have that

$$\begin{aligned}
&\dot{X}\,|_{X=0}=\lambda>0, \quad \dot{Y}\,|_{Y=0}=\beta_V XV\geq 0 \text{ for all } X,V\geq 0,\\
&\dot{I}\,|_{I=0}=\beta_P XP\geq 0 \text{ for all } X,P\geq 0, \quad \dot{V}\,|_{V=0}=\kappa_V Y\geq 0 \text{ for all } Y\geq 0,\\
&\dot{P}\,|_{P=0}=\kappa_P I\geq 0 \text{ for all } I\geq 0,\\
&\dot{Z}\,|_{Z=0}=0, \quad \dot{M}\,|_{M=0}=0.
\end{aligned}$$

This guarantees that $(X(t),Y(t),I(t),V(t),P(t),Z(t),M(t))\in\mathbb{R}^7_{\geq 0}$ for all $t\geq 0$ when $(X(0),Y(0),I(0),V(0),P(0),Z(0),M(0))\in\mathbb{R}^7_{\geq 0}$. Let us define

$$\Psi = X+Y+I+\frac{\gamma_Y}{2\kappa_V}V+\frac{\gamma_I}{2\kappa_P}P+\frac{\gamma_Y\varkappa_V}{2\kappa_V\sigma_Z}Z+\frac{\gamma_I\varkappa_P}{2\kappa_P\sigma_M}M.$$

Then,

$$\begin{aligned}
\dot{\Psi} &= \lambda-\alpha X-\frac{\gamma_Y}{2}Y-\frac{\gamma_I}{2}I-\frac{\gamma_Y\pi_V}{2\kappa_V}V-\frac{\gamma_I\pi_P}{2\kappa_P}P-\frac{\gamma_Y\varkappa_V\mu_Z}{2\kappa_V\sigma_Z}Z-\frac{\gamma_I\varkappa_P\mu_M}{2\kappa_P\sigma_M}M\\
&\leq \lambda-\phi\left[X+Y+I+\frac{\gamma_Y}{2\kappa_V}V+\frac{\gamma_I}{2\kappa_P}P+\frac{\gamma_Y\varkappa_V}{2\kappa_V\sigma_Z}Z+\frac{\gamma_I\varkappa_P}{2\kappa_P\sigma_M}M\right]=\lambda-\phi\Psi,
\end{aligned}$$

where $\phi=\min\{\alpha,\frac{\gamma_Y}{2},\frac{\gamma_I}{2},\pi_V,\pi_P,\mu_Z,\mu_M\}$. Thus, $0\leq\Psi(t)\leq\Delta_1$ if $\Psi(0)\leq\Delta_1$ for $t\geq 0$, where $\Delta_1=\frac{\lambda}{\phi}$. Since X,Y,I,V,P,Z and M are all nonnegative, then $0\leq X(t),Y(t),I(t)\leq\Delta_1$, $0\leq V(t)\leq\Delta_2$, $0\leq P(t)\leq\Delta_3$, $0\leq Z(t)\leq\Delta_4$, $0\leq M(t)\leq\Delta_5$ if $X(0)+Y(0)+I(0)+\frac{\gamma_Y}{2\kappa_V}V(0)+\frac{\gamma_I}{2\kappa_P}P(0)+\frac{\gamma_Y\varkappa_V}{2\kappa_V\sigma_Z}Z(0)+\frac{\gamma_I\varkappa_P}{2\kappa_P\sigma_M}M(0)\leq\Delta_1$, where $\Delta_2=\frac{2\kappa_V}{\gamma_Y}\Delta_1$, $\Delta_3=\frac{2\kappa_P}{\gamma_I}\Delta_1$, $\Delta_4=\frac{2\kappa_V\sigma_Z}{\gamma_Y\varkappa_V}\Delta_1$ and $\Delta_5=\frac{2\kappa_P\sigma_M}{\gamma_I\varkappa_P}\Delta_1$. This proves the boundedness of the solutions. □

4. Equilibria

In this section, we are interested in the conditions of existence of the system's equilibria. Moreover, we derive a set of threshold parameters which govern the existence of equilibria. At any equilibrium $\Xi=(X,Y,I,V,P,Z,M)$, the following equations hold:

$$0=\lambda-\alpha X-\beta_V XV-\beta_P XP, \tag{4}$$
$$0=\beta_V XV-\gamma_Y Y, \tag{5}$$
$$0=\beta_P XP-\gamma_I I, \tag{6}$$
$$0=\kappa_V Y-\pi_V V-\varkappa_V VZ, \tag{7}$$
$$0=\kappa_P I-\pi_P P-\varkappa_P PM, \tag{8}$$
$$0=\sigma_Z VZ-\mu_Z Z, \tag{9}$$
$$0=\sigma_M PM-\mu_M M. \tag{10}$$

Solving Equations (4)–(10), we obtain eight equilibria.

(i) Infection-free equilibrium, $\Xi_0=(X_0,0,0,0,0,0,0)$, where $X_0=\lambda/\alpha$.

(ii) SARS-CoV-2 single-infection equilibrium without antibody immunity $\Xi_1=(X_1,Y_1,0,V_1,0,0,0)$, where

$$X_1=\frac{\gamma_Y\pi_V}{\kappa_V\beta_V},\ Y_1=\frac{\alpha\pi_V}{\kappa_V\beta_V}\left[\frac{X_0\kappa_V\beta_V}{\pi_V\gamma_Y}-1\right],\ V_1=\frac{\alpha}{\beta_V}\left[\frac{X_0\kappa_V\beta_V}{\pi_V\gamma_Y}-1\right]$$

Therefore, $Y_1>0$ and $V_1>0$ when

$$\frac{X_0\kappa_V\beta_V}{\pi_V\gamma_Y}>1.$$

We define the basic SARS-CoV-2 single-infection reproductive ratio as:

$$\Re_1 = \frac{X_0 \kappa_V \beta_V}{\pi_V \gamma_Y}.$$

The parameter $\Re_1$ determines whether or not a SARS-CoV-2 single-infection can be established. Thus, we can write

$$X_1 = \frac{X_0}{\Re_1}, \;\; Y_1 = \frac{\alpha \pi_V}{\kappa_V \beta_V}(\Re_1 - 1), \;\; V_1 = \frac{\alpha}{\beta_V}(\Re_1 - 1).$$

It follows that, Ξ_1 exists if $\Re_1 > 1$.

(iii) IAV single-infection equilibrium without antibody immunity, $\Xi_2 = (X_2, 0, I_2, 0, P_2, 0, 0)$, where

$$X_2 = \frac{\gamma_I \pi_P}{\kappa_P \beta_P}, \;\; I_2 = \frac{\alpha \pi_P}{\kappa_P \beta_P}\left[\frac{X_0 \kappa_P \beta_P}{\pi_P \gamma_I} - 1\right], \;\; P_2 = \frac{\alpha}{\beta_P}\left[\frac{X_0 \kappa_P \beta_P}{\pi_P \gamma_I} - 1\right].$$

Therefore, $I_2 > 0$ and $P_2 > 0$ when

$$\frac{X_0 \kappa_P \beta_P}{\pi_P \gamma_I} > 1.$$

We define the basic IAV-infection reproductive ratio as:

$$\Re_2 = \frac{X_0 \kappa_P \beta_P}{\pi_P \gamma_I}.$$

The parameter $\Re_2$ determines whether or not the IAV single-infection can be established. In terms of $\Re_2$, we can write

$$X_2 = \frac{X_0}{\Re_2}, \;\; I_2 = \frac{\alpha \pi_P}{\kappa_P \beta_P}(\Re_2 - 1), \;\; P_2 = \frac{\alpha}{\beta_P}(\Re_2 - 1).$$

Therefore, Ξ_2 exists if $\Re_2 > 1$.

(iv) SARS-CoV-2 single-infection equilibrium with stimulated SARS-CoV-2-specific antibody immunity, $\Xi_3 = (X_3, Y_3, 0, V_3, 0, Z_3, 0)$, where

$$X_3 = \frac{\lambda \sigma_Z}{\beta_V \mu_Z + \alpha \sigma_Z}, \;\; Y_3 = \frac{\lambda \beta_V \mu_Z}{\gamma_Y(\beta_V \mu_Z + \alpha \sigma_Z)},$$
$$V_3 = \frac{\mu_Z}{\sigma_Z}, \;\; Z_3 = \frac{\pi_V}{\varkappa_V}\left[\frac{\lambda \beta_V \sigma_Z \kappa_V}{\gamma_Y \pi_V(\beta_V \mu_Z + \alpha \sigma_Z)} - 1\right].$$

We note that Ξ_3 exists when

$$\frac{\lambda \beta_V \sigma_Z \kappa_V}{\gamma_Y \pi_V(\beta_V \mu_Z + \alpha \sigma_Z)} > 1.$$

The SARS-CoV-2-specific antibody activation ratio in case of SARS-CoV-2 single-infection is stated as:

$$\Re_3 = \frac{\lambda \beta_V \sigma_Z \kappa_V}{\gamma_Y \pi_V(\beta_V \mu_Z + \alpha \sigma_Z)}.$$

Thus, $Z_3 = \frac{\pi_V}{\varkappa_V}(\Re_3 - 1)$. The parameter $\Re_3$ determines whether or not the SARS-CoV-2-specific antibody immunity is activated in the absence of IAV infection.

(v) IAV single-infection equilibrium with stimulated IAV-specific antibody immunity, $\Xi_4 = (X_4, 0, I_4, 0, P_4, 0, M_4)$, where

$$X_4 = \frac{\lambda\sigma_M}{\beta_P\mu_M + \alpha\sigma_M}, \quad I_4 = \frac{\lambda\beta_P\mu_M}{\gamma_I(\beta_P\mu_M + \alpha\sigma_M)},$$
$$P_4 = \frac{\mu_M}{\sigma_M}, \quad M_4 = \frac{\pi_P}{\varkappa_P}\left[\frac{\lambda\beta_P\sigma_M\kappa_P}{\gamma_I\pi_P(\beta_P\mu_M + \alpha\sigma_M)} - 1\right].$$

We note that Ξ_4 exists when

$$\frac{\lambda\beta_P\sigma_M\kappa_P}{\gamma_I\pi_P(\beta_P\mu_M + \alpha\sigma_M)} > 1.$$

The IAV-specific antibody immunity activation ratio for IAV single-infection is stated as:

$$\Re_4 = \frac{\lambda\beta_P\sigma_M\kappa_P}{\gamma_I\pi_P(\beta_P\mu_M + \alpha\sigma_M)}.$$

Thus, $M_4 = \frac{\pi_P}{\varkappa_P}(\Re_4 - 1)$. The parameter $\Re_4$ determines whether or not the IAV-specific antibody immunity is activated in the absence of SARS-CoV-2 infection.

(vi) IAV/SARS-CoV-2 coinfection equilibrium with only stimulated SARS-CoV-2-specific antibody immunity, $\Xi_5 = (X_5, Y_5, I_5, V_5, P_5, Z_5, 0)$, where

$$X_5 = \frac{\gamma_I\pi_P}{\kappa_P\beta_P} = X_2, \quad Y_5 = \frac{\beta_V\mu_Z}{\gamma_Y\sigma_Z}X_5,$$
$$I_5 = \frac{\pi_P(\beta_V\mu_Z + \alpha\sigma_Z)}{\beta_P\sigma_Z\kappa_P}\left[\frac{\lambda\beta_P\kappa_P\sigma_Z}{\gamma_I\pi_P(\beta_V\mu_Z + \alpha\sigma_Z)} - 1\right], \quad V_5 = \frac{\mu_Z}{\sigma_Z} = V_3,$$
$$P_5 = \frac{\beta_V\mu_Z + \alpha\sigma_Z}{\beta_P\sigma_Z}\left[\frac{\lambda\beta_P\kappa_P\sigma_Z}{\gamma_I\pi_P(\beta_V\mu_Z + \alpha\sigma_Z)} - 1\right],$$
$$Z_5 = \frac{\pi_V}{\varkappa_V}\left[\frac{\pi_P\beta_V\kappa_V\gamma_I}{\pi_V\beta_P\kappa_P\gamma_Y} - 1\right] = \frac{\pi_V}{\varkappa_V}(\Re_1/\Re_2 - 1).$$

We note that Ξ_5 exists when,

$$\frac{\Re_1}{\Re_2} > 1 \text{ and } \frac{\lambda\beta_P\kappa_P\sigma_Z}{\gamma_I\pi_P(\beta_V\mu_Z + \alpha\sigma_Z)} > 1.$$

The SARS-CoV-2 infection reproductive ratio in the presence of IAV infection is stated as:

$$\Re_5 = \frac{\lambda\beta_P\kappa_P\sigma_Z}{\gamma_I\pi_P(\beta_V\mu_Z + \alpha\sigma_Z)}.$$

The parameter $\Re_5$ determines whether or not SARS-CoV-2 infected patients could be coinfected with IAV. Hence,

$$I_5 = \frac{\pi_P(\beta_V\mu_Z + \alpha\sigma_Z)}{\beta_P\sigma_Z\kappa_P}(\Re_5 - 1), \quad P_5 = \frac{\beta_V\mu_Z + \alpha\sigma_Z}{\beta_P\sigma_Z}(\Re_5 - 1).$$

and then Ξ_5 exists if $\frac{\Re_1}{\Re_2} > 1$ and $\Re_5 > 1$.

(vii) IAV/SARS-CoV-2 coinfection equilibrium with only stimulated IAV-specific antibody immunity, $\Xi_6 = (X_6, Y_6, I_6, V_6, P_6, 0, M_6)$, where

$$X_6 = \frac{\gamma_Y \pi_V}{\kappa_V \beta_V}, \quad Y_6 = \frac{\pi_V(\beta_P \mu_M + \alpha\sigma_M)}{\beta_V \sigma_M \kappa_V}\left[\frac{\lambda\beta_V\kappa_V\sigma_M}{\gamma_Y\pi_V(\beta_P\mu_M + \alpha\sigma_M)} - 1\right],$$
$$I_6 = \frac{\pi_V\beta_P\gamma_Y\mu_M}{\beta_V\kappa_V\gamma_I\sigma_M}, \quad V_6 = \frac{\beta_P\mu_M + \alpha\sigma_M}{\beta_V\sigma_M}\left[\frac{\lambda\beta_V\kappa_V\sigma_M}{\gamma_Y\pi_V(\beta_P\mu_M + \alpha\sigma_M)} - 1\right],$$
$$P_6 = \frac{\mu_M}{\sigma_M} = P_4, \quad M_6 = \frac{\pi_P}{\varkappa_P}\left[\frac{\pi_V\beta_P\kappa_P\gamma_Y}{\pi_P\beta_V\kappa_V\gamma_I} - 1\right] = \frac{\pi_P}{\varkappa_P}(\Re_2/\Re_1 - 1).$$

We note that Ξ_6 exists when

$$\frac{\Re_2}{\Re_1} > 1 \text{ and } \frac{\lambda\beta_V\kappa_V\sigma_M}{\gamma_Y\pi_V(\beta_P\mu_M + \alpha\sigma_M)} > 1.$$

The SARS-CoV-2 infection reproductive ratio in the presence of IAV infection is stated as:

$$\Re_6 = \frac{\lambda\beta_V\kappa_V\sigma_M}{\gamma_Y\pi_V(\beta_P\mu_M + \alpha\sigma_M)}.$$

Thus,

$$Y_6 = \frac{\pi_V(\beta_P\mu_M + \alpha\sigma_M)}{\beta_V\sigma_M\kappa_V}(\Re_6 - 1), \quad V_6 = \frac{\beta_P\mu_M + \alpha\sigma_M}{\beta_V\sigma_M}(\Re_6 - 1).$$

The parameter $\Re_6$ determines whether or not SARS-CoV-2 infected patients could be coinfected with IAV.

(viii) IAV/SARS-CoV-2 coinfection equilibrium with stimulated both SARS-CoV-2-specific and IAV-specific antibody immunities $\Xi_7 = (X_7, Y_7, I_7, V_7, P_7, Z_7, M_7)$, where

$$X_7 = \frac{\lambda\sigma_Z\sigma_M}{\beta_P\mu_M\sigma_Z + \beta_V\mu_Z\sigma_M + \alpha\sigma_Z\sigma_M}, \quad Y_7 = \frac{\beta_V\lambda\mu_Z\sigma_M}{\gamma_Y(\beta_P\mu_M\sigma_Z + \beta_V\mu_Z\sigma_M + \alpha\sigma_Z\sigma_M)},$$
$$I_7 = \frac{\beta_P\lambda\mu_M\sigma_Z}{\gamma_I(\beta_P\mu_M\sigma_Z + \beta_V\mu_Z\sigma_M + \alpha\sigma_Z\sigma_M)}, \quad V_7 = \frac{\mu_Z}{\sigma_Z} = V_3, \quad P_7 = \frac{\mu_M}{\sigma 2} = P_4,$$
$$Z_7 = \frac{\pi_V}{\varkappa_V}\left[\frac{\lambda\beta_V\kappa_V\sigma_M\sigma_Z}{\gamma_Y\pi_V(\beta_P\mu_M\sigma_Z + \beta_V\mu_Z\sigma_M + \alpha\sigma_Z\sigma_M)} - 1\right],$$
$$M_7 = \frac{\pi_P}{\varkappa_P}\left[\frac{\lambda\beta_P\kappa_P\sigma_M\sigma_Z}{\gamma_I\pi_P(\beta_P\mu_M\sigma_Z + \beta_V\mu_Z\sigma_M + \alpha\sigma_Z\sigma_M)} - 1\right].$$

It is obvious that Ξ_7 exists when

$$\frac{\lambda\beta_P\kappa_P\sigma_M\sigma_Z}{\gamma_I\pi_P(\beta_P\mu_M\sigma_Z + \beta_V\mu_Z\sigma_M + \alpha\sigma_Z\sigma_M)} > 1,$$
$$\frac{\lambda\beta_V\kappa_V\sigma_M\sigma_Z}{\gamma_Y\pi_V(\beta_P\mu_M\sigma_Z + \beta_V\mu_Z\sigma_M + \alpha\sigma_Z\sigma_M)} > 1.$$

Now, we define

$$\Re_7 = \frac{\lambda\beta_P\kappa_P\sigma_M\sigma_Z}{\gamma_I\pi_P(\beta_P\mu_M\sigma_Z + \beta_V\mu_Z\sigma_M + \alpha\sigma_Z\sigma_M)},$$
$$\Re_8 = \frac{\lambda\beta_V\kappa_V\sigma_M\sigma_Z}{\gamma_Y\pi_V(\beta_P\mu_M\sigma_Z + \beta_V\mu_Z\sigma_M + \alpha\sigma_Z\sigma_M)}.$$

Here, $\Re_7$ is the SARS-CoV-2-specific antibody activation ratio in case of IAV/SARS-CoV-2 coinfection, and $\Re_8$ is the IAV-specific antibody activation ratio in case of IAV/SARS-CoV-2 coinfection.

Hence, $M_7 = \frac{\pi_P}{\varkappa_P}(\Re_7 - 1)$ and $Z_7 = \frac{\pi_V}{\varkappa_V}(\Re_8 - 1)$. If $\Re_7 > 1$ and $\Re_8 > 1$, then Ξ_7 exists.

In summary, we have eight threshold parameters which determine the existence of the model's equilibria

$$\begin{aligned}
\Re_1 &= \frac{X_0\kappa_V\beta_V}{\pi_V\gamma_Y}, \quad \Re_2 = \frac{X_0\kappa_P\beta_P}{\pi_P\gamma_I}, \quad \Re_3 = \frac{\lambda\beta_V\sigma_Z\kappa_V}{\gamma_Y\pi_V(\beta_V\mu_Z+\alpha\sigma_Z)},\\
\Re_4 &= \frac{\lambda\beta_P\sigma_M\kappa_P}{\gamma_I\pi_P(\beta_P\mu_M+\alpha\sigma_M)}, \quad \Re_5 = \frac{\lambda\beta_P\kappa_P\sigma_Z}{\gamma_I\pi_P(\beta_V\mu_Z+\alpha\sigma_Z)},\\
\Re_6 &= \frac{\lambda\beta_V\kappa_V\sigma_M}{\gamma_Y\pi_V(\beta_P\mu_M+\alpha\sigma_M)}, \quad \Re_7 = \frac{\lambda\beta_P\kappa_P\sigma_M\sigma_Z}{\gamma_I\pi_P(\beta_P\mu_M\sigma_Z+\beta_V\mu_Z\sigma_M+\alpha\sigma_Z\sigma_M)},\\
\Re_8 &= \frac{\lambda\beta_V\kappa_V\sigma_M\sigma_Z}{\gamma_Y\pi_V(\beta_P\mu_M\sigma_Z+\beta_V\mu_Z\sigma_M+\alpha\sigma_Z\sigma_M)}.
\end{aligned} \tag{11}$$

5. Global Stability

Stability analysis is at the heart of dynamical analysis. Only stable solutions can be noticed experimentally. Therefore, in this section we examine the global asymptotic stability of all equilibria by establishing suitable Lyapunov functions [58] and applying the Lyapunov–LaSalle asymptotic stability theorem (L-LAST) [59–61]. The following arithmetic-mean-geometric-mean inequality will be utilized:

$$\frac{u_1+u_2+\cdots+u_n}{n} \geq \sqrt[n]{(u_1)(u_2)\ldots(u_n)}. \tag{12}$$

Let a function $\Lambda_j(X,Y,I,V,P,Z,M)$ and $\tilde{\Omega}_j$ be the largest invariant subset of

$$\Omega_j = \left\{(X,Y,I,V,P,Z,M) : \frac{d\Lambda_j}{dt} = 0\right\}, \quad j = 0,1,2,\ldots,7.$$

Define a function

$$F(v) = v - 1 - \ln v.$$

The following result suggests that when $\Re_1 \leq 1$ and $\Re_2 \leq 1$, both IAV and SARS-CoV-2 infections are predicted to die out regardless of the initial conditions (any disease stages).

Theorem 1. *If $\Re_1 \leq 1$ and $\Re_2 \leq 1$, then Ξ_0 is globally asymptotically stable (G.A.S).*

Proof. Define

$$\Lambda_0 = X_0 F\left(\frac{X}{X_0}\right) + Y + I + \frac{\gamma_Y}{\kappa_V}V + \frac{\gamma_I}{\kappa_P}P + \frac{\gamma_Y\varkappa_V}{\kappa_V\sigma_Z}Z + \frac{\gamma_I\varkappa_P}{\kappa_P\sigma_M}M.$$

We note that $\Lambda_0 > 0$ for all $X,Y,I,V,P,Z,M > 0$, and $\Lambda_0(X_0,0,0,0,0,0,0) = 0$. □

We calculate $\frac{d\Lambda_0}{dt}$ along the solutions of model (3) as:

$$\begin{aligned}
\frac{d\Lambda_0}{dt} &= \left(1-\frac{X_0}{X}\right)[\lambda - \alpha X - \beta_V XV - \beta_P XP] + \beta_V XV - \gamma_Y Y + \beta_P XP - \gamma_I I\\
&+ \frac{\gamma_Y}{\kappa_V}[\kappa_V Y - \pi_V V - \varkappa_V VZ] + \frac{\gamma_I}{\kappa_P}[\kappa_P I - \pi_P P - \varkappa_P PM] + \frac{\gamma_Y\varkappa_V}{\kappa_V\sigma_Z}[\sigma_Z VZ - \mu_Z Z]\\
&+ \frac{\gamma_I\varkappa_P}{\kappa_P\sigma_M}[\sigma_M PM - \mu_M M]\\
&= \left(1-\frac{X_0}{X}\right)(\lambda - \alpha X) + \beta_V X_0 V + \beta_P X_0 P - \frac{\gamma_Y\pi_V}{\kappa_V}V - \frac{\gamma_I\pi_P}{\kappa_P}P - \frac{\gamma_Y\varkappa_V\mu_Z}{\kappa_V\sigma_Z}Z - \frac{\gamma_I\varkappa_P\mu_M}{\kappa_P\sigma_M}M.
\end{aligned}$$

Using the equilibrium condition $\lambda = \alpha X_0$, we obtain:

$$\frac{d\Lambda_0}{dt} = -\alpha\frac{(X-X_0)^2}{X} + \frac{\gamma_Y\pi_V}{\kappa_V}(\Re_1 - 1)V + \frac{\gamma_I\pi_P}{\kappa_P}(\Re_2 - 1)P - \frac{\gamma_Y\varkappa_V\mu_Z}{\kappa_V\sigma_Z}Z - \frac{\gamma_I\varkappa_P\mu_M}{\kappa_P\sigma_M}M.$$

Since $\Re_1 \leq 1$ and $\Re_2 \leq 1$, then $\frac{d\Lambda_0}{dt} \leq 0$ for all $X, V, P, Z, M > 0$. In addition, $\frac{d\Lambda_0}{dt} = 0$ when $X = X_0$ and $V = P = Z = M = 0$. The solutions of system (3) tend to $\tilde{\Omega}_0$ [62] which includes elements with $V = P = 0$. Thus, $\dot{V} = \dot{P} = 0$ and from the fourth and fifth equations of system (3) we have:

$$0 = \dot{V} = \kappa_V Y \Longrightarrow Y(t) = 0, \text{ for all } t$$
$$0 = \dot{P} = \kappa_P I \Longrightarrow I(t) = 0, \text{ for all } t.$$

Therefore, $\tilde{\Omega}_0 = \{\Xi_0\}$ and applying L-LAST [59–61], we obtain that Ξ_0 is G.A.S.

The following result suggests that, when $\Re_1 > 1$, $\Re_2/\Re_1 \leq 1$ and $\Re_3 \leq 1$, the SARS-CoV-2 single-infection with inactive immune response is always established regardless of the initial conditions.

Theorem 2. *Suppose that* $\Re_1 > 1$, $\Re_2/\Re_1 \leq 1$ *and* $\Re_3 \leq 1$, *then* Ξ_1 *is G.A.S* .

Proof. Let us formulate a Lyapunov function Λ_1 as:

$$\Lambda_1 = X_1 F\left(\frac{X}{X_1}\right) + Y_1 F\left(\frac{Y}{Y_1}\right) + I + \frac{\gamma_Y}{\kappa_V} V_1 F\left(\frac{V}{V_1}\right) + \frac{\gamma_I}{\kappa_P} P + \frac{\gamma_Y \varkappa_V}{\kappa_V \sigma_Z} Z + \frac{\gamma_I \varkappa_P}{\kappa_P \sigma_M} M.$$

□

We calculate $\frac{d\Lambda_1}{dt}$ as:

$$\begin{aligned}\frac{d\Lambda_1}{dt} &= \left(1 - \frac{X_1}{X}\right)[\lambda - \alpha X - \beta_V XV - \beta_P XP] + \left(1 - \frac{Y_1}{Y}\right)[\beta_V XV - \gamma_Y Y] + \beta_P XP - \gamma_I I \\ &+ \frac{\gamma_Y}{\kappa_V}\left(1 - \frac{V_1}{V}\right)[\kappa_V Y - \pi_V V - \varkappa_V VZ] + \frac{\gamma_I}{\kappa_P}[\kappa_P I - \pi_P P - \varkappa_P PM] \\ &+ \frac{\gamma_Y \varkappa_V}{\kappa_V \sigma_Z}[\sigma_Z VZ - \mu_Z Z] + \frac{\gamma_I \varkappa_P}{\kappa_P \sigma_M}[\sigma_M PM - \mu_M M]. \end{aligned} \tag{13}$$

Simplifying Equation (13), we obtain:

$$\begin{aligned}\frac{d\Lambda_1}{dt} &= \left(1 - \frac{X_1}{X}\right)(\lambda - \alpha X) + \beta_V X_1 V + \beta_P X_1 P - \beta_V XV\frac{Y_1}{Y} + \gamma_Y Y_1 - \frac{\gamma_Y \pi_V}{\kappa_V} V \\ &- \gamma_Y Y \frac{V_1}{V} + \frac{\gamma_Y \pi_V}{\kappa_V} V_1 + \frac{\gamma_Y \varkappa_V}{\kappa_V} V_1 Z - \frac{\gamma_I \pi_P}{\kappa_P} P - \frac{\gamma_Y \varkappa_V \mu_Z}{\kappa_V \sigma_Z} Z - \frac{\gamma_I \varkappa_P \mu_M}{\kappa_P \sigma_M} M.\end{aligned}$$

Using the equilibrium conditions for Ξ_1:

$$\lambda = \alpha X_1 + \beta_V X_1 V_1, \quad \beta_V X_1 V_1 = \gamma_Y Y_1, \quad Y_1 = \frac{\pi_V}{\kappa_V} V_1,$$

we obtain

$$\begin{aligned}\frac{d\Lambda_1}{dt} &= \left(1 - \frac{X_1}{X}\right)(\alpha X_1 - \alpha X) + 3\beta_V X_1 V_1 - \beta_V X_1 V_1 \frac{X_1}{X} - \beta_V X_1 V_1 \frac{Y_1 XV}{Y X_1 V_1} \\ &- \beta_V X_1 V_1 \frac{V_1 Y}{V Y_1} + \frac{\gamma_I \pi_P}{\kappa_P}\left(\frac{\beta_P X_1 \kappa_P}{\gamma_I \pi_P} - 1\right) P + \frac{\gamma_Y \varkappa_V \mu_Z}{\kappa_V \sigma_Z}\left(\frac{\sigma_Z}{\mu_Z} V_1 - 1\right) Z \\ &- \frac{\gamma_I \varkappa_P \mu_M}{\kappa_P \sigma_M} M.\end{aligned} \tag{14}$$

Then, collecting terms of (14), we obtain:

$$\frac{d\Lambda_1}{dt} = -\frac{\alpha(X-X_1)^2}{X} + \beta_V X_1 V_1\left(3 - \frac{X_1}{X} - \frac{Y_1 XV}{YX_1V_1} - \frac{V_1 Y}{VY_1}\right) + \frac{\gamma_I \pi_P}{\kappa_P}\left(\frac{\Re_2}{\Re_1} - 1\right)P + \frac{\gamma_Y \varkappa_V(\alpha\sigma_Z + \beta_V\mu_Z)}{\kappa_V\beta_V\sigma_Z}(\Re_3 - 1)Z - \frac{\gamma_I\varkappa_P\mu_M}{\kappa_P\sigma_M}M.$$

Using inequality (12), we obtain:

$$3 - \frac{X_1}{X} - \frac{Y_1XV}{YX_1V_1} - \frac{V_1Y}{VY_1} \leq 0.$$

Since $\Re_2/\Re_1 \leq 1$ and $\Re_3 \leq 1$ then, $\frac{d\Lambda_1}{dt} \leq 0$ for all $X, Y, V, P, Z, M > 0$. Moreover, $\frac{d\Lambda_1}{dt} = 0$ when $X = X_1$, $Y = Y_1$, $V = V_1$, and $P = Z = M = 0$. The solutions of system (3) tend to $\tilde{\Omega}_1$ where $P = 0$. Hence, $\dot{P} = 0$, and the fifth equation of system (3) gives

$$0 = \dot{P} = \kappa_P I \Longrightarrow I(t) = 0, \text{ for all } t.$$

Hence, $\tilde{\Omega}_1 = \{\Xi_1\}$ and Ξ_1 is G.A.S. by using L-LAST [59–61].

The result of the following theorem suggests that, when $\Re_2 > 1$, $\Re_1/\Re_2 \leq 1$ and $\Re_4 \leq 1$, the IAV single-infection with inactive immune response is always established regardless of the initial conditions.

Theorem 3. *Let* $\Re_2 > 1$, $\Re_1/\Re_2 \leq 1$ *and* $\Re_4 \leq 1$, *then* Ξ_2 *is G.A.S.*

Proof. Consider

$$\Lambda_2 = X_2 F\left(\frac{X}{X_2}\right) + Y + I_2 F\left(\frac{I}{I_2}\right) + \frac{\gamma_Y}{\kappa_V}V + \frac{\gamma_I}{\kappa_P}P_2 F\left(\frac{P}{P_2}\right) + \frac{\gamma_Y\varkappa_V}{\kappa_V\sigma_Z}Z + \frac{\gamma_I\varkappa_P}{\kappa_P\sigma_M}M.$$

□

We calculate $\frac{d\Lambda_2}{dt}$ as:

$$\begin{aligned}\frac{d\Lambda_2}{dt} &= \left(1 - \frac{X_2}{X}\right)[\lambda - \alpha X - \beta_V XV - \beta_P XP] + \beta_V XV - \gamma_Y Y + \left(1 - \frac{I_2}{I}\right)[\beta_P XP - \gamma_I I] \\ &+ \frac{\gamma_Y}{\kappa_V}[\kappa_V Y - \pi_V V - \varkappa_V VZ] + \frac{\gamma_I}{\kappa_P}\left(1 - \frac{P_2}{P}\right)[\kappa_P I - \pi_P P - \varkappa_P PM] \\ &+ \frac{\gamma_Y\varkappa_V}{\kappa_V\sigma_Z}[\sigma_Z VZ - \mu_Z Z] + \frac{\gamma_I\varkappa_P}{\kappa_P\sigma_M}[\sigma_M PM - \mu_M M]. \end{aligned} \quad (15)$$

Then, simplifying Equation (15), we obtain:

$$\begin{aligned}\frac{d\Lambda_2}{dt} &= \left(1 - \frac{X_2}{X}\right)(\lambda - \alpha X) + \beta_V X_2 V + \beta_P X_2 P - \beta_P XP\frac{I_2}{I} + \gamma_I I_2 - \frac{\gamma_Y\pi_V}{\kappa_V}V - \frac{\gamma_I\pi_P}{\kappa_P}P \\ &- \gamma_I I\frac{P_2}{P} + \frac{\gamma_I\pi_P}{\kappa_P}P_2 + \frac{\gamma_I\varkappa_P}{\kappa_P}P_2M - \frac{\gamma_Y\varkappa_V\mu_Z}{\kappa_V\sigma_Z}Z - \frac{\gamma_I\varkappa_P\mu_M}{\kappa_P\sigma_M}M.\end{aligned}$$

Using the equilibrium conditions for Ξ_2:

$$\lambda = \alpha X_2 + \beta_P X_2 P_2, \quad \beta_P X_2 P_2 = \gamma_I I_2, \quad I_2 = \frac{\pi_P}{\kappa_P}P_2,$$

we obtain,

$$\begin{aligned}\frac{d\Lambda_2}{dt} &= \left(1-\frac{X_2}{X}\right)(\alpha X_2-\alpha X)+3\beta_P X_2P_2-\beta_P X_2P_2\frac{X_2}{X}-\beta_P X_2P_2\frac{I_2XP}{IX_2P_2}\\ &\quad-\beta_P X_2P_2\frac{P_2I}{PI_2}+\frac{\gamma_Y\pi_V}{\kappa_V}\left(\frac{\beta_V X_2\kappa_V}{\gamma_Y\pi_V}-1\right)V+\frac{\gamma_I\varkappa_P\mu_M}{\kappa_P\sigma_M}\left(\frac{\sigma_M}{\mu_M}P_2-1\right)M-\frac{\gamma_Y\varkappa_V\mu_Z}{\kappa_V\sigma_Z}Z\\ &= -\frac{\alpha(X-X_2)^2}{X}+\beta_P X_2P_2\left(3-\frac{X_2}{X}-\frac{I_2XP}{IX_2P_2}-\frac{P_2I}{PI_2}\right)+\frac{\gamma_Y\pi_V}{\kappa_V}(\Re_1/\Re_2-1)V\\ &\quad+\frac{\gamma_I\varkappa_P(\alpha\sigma_M+\beta_P\mu_M)}{\kappa_P\beta_P\sigma_M}(\Re_4-1)M-\frac{\gamma_Y\varkappa_V\mu_Z}{\kappa_V\sigma_Z}Z.\end{aligned}$$

If $\Re_1/\Re_2 \leq 1$ and $\Re_4 \leq 1$, then employing inequality (12), we obtain $\frac{d\Lambda_2}{dt} \leq 0$ for all $X, I, V, P, Z, M > 0$. Further, $\frac{d\Lambda_2}{dt} = 0$ when $X = X_2$, $I = I_2$, $P = P_2$ and $V = Z = M = 0$. The solutions of system (3) tend to $\tilde{\Omega}_2$ which has $V = 0$ and gives $\dot{V} = 0$. The fourth equation of system (3) gives

$$0 = \dot{V} = \kappa_V Y \Longrightarrow Y(t) = 0, \text{ for all } t.$$

Therefore, $\tilde{\Omega}_2 = \{\Xi_2\}$. Applying L-LAST, we obtain Ξ_2 is G.A.S.

The next result shows that when $\Re_3 > 1$ and $\Re_5 \leq 1$, the SARS-CoV-2 single-infection with active immune response is always established regardless of the initial conditions.

Theorem 4. *Let* $\Re_3 > 1$ *and* $\Re_5 \leq 1$, *then* Ξ_3 *is G.A.S.*

Proof. Define

$$\begin{aligned}\Lambda_3 &= X_3F\left(\frac{X}{X_3}\right)+Y_3F\left(\frac{Y}{Y_3}\right)+I+\frac{\gamma_Y}{\kappa_V}V_3F\left(\frac{V}{V_3}\right)\\ &\quad+\frac{\gamma_I}{\kappa_P}P+\frac{\gamma_Y\varkappa_V}{\kappa_V\sigma_Z}Z_3F\left(\frac{Z}{Z_3}\right)+\frac{\gamma_I\varkappa_P}{\kappa_P\sigma_M}M.\end{aligned}$$

□

We calculate $\frac{d\Lambda_3}{dt}$ as:

$$\begin{aligned}\frac{d\Lambda_3}{dt} &= \left(1-\frac{X_3}{X}\right)[\lambda-\alpha X-\beta_V XV-\beta_P XP]+\left(1-\frac{Y_3}{Y}\right)[\beta_V XV-\gamma_Y Y]+\beta_P XP-\gamma_I I\\ &\quad+\frac{\gamma_Y}{\kappa_V}\left(1-\frac{V_3}{V}\right)[\kappa_V Y-\pi_V V-\varkappa_V VZ]+\frac{\gamma_I}{\kappa_P}[\kappa_P I-\pi_P P-\varkappa_P PM]\\ &\quad+\frac{\gamma_Y\varkappa_V}{\kappa_V\sigma_Z}\left(1-\frac{Z_3}{Z}\right)[\sigma_Z VZ-\mu_Z Z]+\frac{\gamma_I\varkappa_P}{\kappa_P\sigma_M}[\sigma_M PM-\mu_M M].\end{aligned} \tag{16}$$

Then, simplifying Equation (16), we obtain:

$$\begin{aligned}\frac{d\Lambda_3}{dt} &= \left(1-\frac{X_3}{X}\right)(\lambda-\alpha X)+\beta_V X_3V+\beta_P X_3P-\beta_V XV\frac{Y_3}{Y}+\gamma_Y Y_3-\frac{\gamma_Y\pi_V}{\kappa_V}V-\gamma_Y Y\frac{V_3}{V}\\ &\quad+\frac{\gamma_Y\pi_V}{\kappa_V}V_3+\frac{\gamma_Y\varkappa_V}{\kappa_V}V_3Z-\frac{\gamma_I\pi_P}{\kappa_P}P-\frac{\gamma_Y\varkappa_V\mu_Z}{\kappa_V\sigma_Z}Z-\frac{\gamma_Y\varkappa_V}{\kappa_V}Z_3V+\frac{\gamma_Y\varkappa_V\mu_Z}{\kappa_V\sigma_Z}Z_3-\frac{\gamma_I\varkappa_P\mu_M}{\kappa_P\sigma_M}M.\end{aligned}$$

Using the equilibrium conditions for Ξ_3:

$$\begin{aligned}\lambda &= \alpha X_3+\beta_V X_3V_3, \quad \beta_V X_3V_3 = \gamma_Y Y_3,\\ Y_3 &= \frac{\pi_V}{\kappa_V}V_3+\frac{\varkappa_V}{\kappa_V}V_3Z_3,\\ V_3 &= \frac{\mu_Z}{\sigma_Z},\end{aligned}$$

we obtain,

$$\begin{aligned}\frac{d\Lambda_3}{dt} &= \left(1-\frac{X_3}{X}\right)(\alpha X_3-\alpha X)+3\beta_V X_3V_3-\beta_V X_3V_3\frac{X_3}{X}-\beta_V X_3V_3\frac{Y_3XV}{YX_3V_3}\\ &\quad-\beta_V X_3V_3\frac{V_3Y}{VY_3}+\frac{\gamma_I\pi_P}{\kappa_P}\left(\frac{\beta_P X_3\kappa_P}{\gamma_I\pi_P}-1\right)P-\frac{\gamma_I\varkappa_P\mu_M}{\kappa_P\sigma_M}M\\ &= -\frac{\alpha(X-X_3)^2}{X}+\beta_V X_3V_3\left(3-\frac{X_3}{X}-\frac{Y_3XV}{YX_3V_3}-\frac{V_3Y}{VY_3}\right)+\frac{\gamma_I\pi_P}{\kappa_P}(\Re_5-1)P-\frac{\gamma_I\varkappa_P\mu_M}{\kappa_P\sigma_M}M.\end{aligned}$$

Using inequality (12) and $\Re_5 \leq 1$, we obtain $\frac{d\Lambda_3}{dt} \leq 0$ for all $X, Y, V, P, M > 0$. Further, $\frac{d\Lambda_3}{dt} = 0$ when $X = X_3$, $Y = Y_3$, $V = V_3$ and $P = M = 0$. Further, the trajectories of system (3) tend to $\tilde{\Omega}_3$ which has elements with $V = V_3$ and $P = 0$. Then, $\dot{V} = 0$ and $\dot{P} = 0$. The fourth and fifth equations of system (3) provide

$$\begin{aligned}0 = \dot{V} = \kappa_V Y_3 - \pi_V V_3 - \varkappa_V V_3 Z \Longrightarrow Z(t) = Z_3, \text{ for all } t,\\ 0 = \dot{P} = \kappa_P I \Longrightarrow I(t) = 0, \text{ for all } t.\end{aligned}$$

Consequently, $\tilde{\Omega}_3 = \{\Xi_3\}$. Applying L-LAST, we find that Ξ_3 is G.A.S.

In the following theorem, we show that when $\Re_4 > 1$ and $\Re_6 \leq 1$, the IAV single-infection with active immune response is always established regardless of the initial conditions.

Theorem 5. *If* $\Re_4 > 1$ *and* $\Re_6 \leq 1$, *then* Ξ_4 *is G.A.S.*

Proof. Define a function Λ_4 as:

$$\Lambda_4 = X_4 F\left(\frac{X}{X_4}\right)+Y+I_4 F\left(\frac{I}{I_4}\right)+\frac{\gamma_Y}{\kappa_V}V+\frac{\gamma_I}{\kappa_P}P_4 F\left(\frac{P}{P_4}\right)+\frac{\gamma_Y\varkappa_V}{\kappa_V\sigma_Z}Z+\frac{\gamma_I\varkappa_P}{\kappa_P\sigma_M}M_4 F\left(\frac{M}{M_4}\right).$$

□

Calculating $\frac{d\Lambda_4}{dt}$ as:

$$\begin{aligned}\frac{d\Lambda_4}{dt} &= \left(1-\frac{X_4}{X}\right)[\lambda-\alpha X-\beta_V XV-\beta_P XP]+\beta_V XV-\gamma_Y Y+\left(1-\frac{I_4}{I}\right)[\beta_P XP-\gamma_I I]\\ &\quad+\frac{\gamma_Y}{\kappa_V}[\kappa_V Y-\pi_V V-\varkappa_V VZ]+\frac{\gamma_I}{\kappa_P}\left(1-\frac{P_4}{P}\right)[\kappa_P I-\pi_P P-\varkappa_P PM]\\ &\quad+\frac{\gamma_Y\varkappa_V}{\kappa_V\sigma_Z}[\sigma_Z VZ-\mu_Z Z]+\frac{\gamma_I\varkappa_P}{\kappa_P\sigma_M}\left(1-\frac{M_4}{M}\right)[\sigma_M PM-\mu_M M].\end{aligned} \tag{17}$$

Equation (17) can be written as:

$$\begin{aligned}\frac{d\Lambda_4}{dt} &= \left(1-\frac{X_4}{X}\right)(\lambda-\alpha X)+\beta_V X_4V+\beta_P X_4P-\beta_P XP\frac{I_2}{I}+\gamma_I I_4-\frac{\gamma_Y\pi_V}{\kappa_V}V\\ &\quad-\frac{\gamma_I\pi_P}{\kappa_P}P-\gamma_I I\frac{P_4}{P}+\frac{\gamma_I\pi_P}{\kappa_P}P_4+\frac{\gamma_I\varkappa_P}{\kappa_P}P_4M-\frac{\gamma_Y\varkappa_V\mu_Z}{\kappa_V\sigma_Z}Z-\frac{\gamma_I\varkappa_P\mu_M}{\kappa_P\sigma_M}M\\ &\quad-\frac{\gamma_I\varkappa_P}{\kappa_P}M_4P+\frac{\gamma_I\varkappa_P\mu_M}{\kappa_P\sigma_M}M_4.\end{aligned}$$

Using the equilibrium conditions for Ξ_4:

$$\begin{aligned}\lambda = \alpha X_4+\beta_P X_4P_4, \quad \beta_P X_4P_4 = \gamma_I I_4,\\ I_4 = \frac{\pi_P}{\kappa_P}P_4+\frac{\varkappa_P}{\kappa_P}P_4M_4, \quad P_4 = \frac{\mu_M}{\sigma_M},\end{aligned}$$

we obtain,

$$\begin{aligned}\frac{d\Lambda_4}{dt} &= \left(1-\frac{X_4}{X}\right)(\alpha X_4-\alpha X)+3\beta_P X_4P_4-\beta_P X_4P_4\frac{X_4}{X}-\beta_P X_4P_4\frac{I_4XP}{IX_4P_4}\\ &\quad-\beta_P X_4P_4\frac{P_4I}{PI_4}+\frac{\gamma_Y\pi_V}{\kappa_V}\left(\frac{\beta_V X_4\kappa_V}{\gamma_Y\pi_V}-1\right)V-\frac{\gamma_Y\varkappa_V\mu_Z}{\kappa_V\sigma_Z}Z\\ &= -\frac{\alpha(X-X_4)^2}{X}+\beta_P X_4P_4\left(3-\frac{X_4}{X}-\frac{I_4XP}{IX_4P_4}-\frac{P_4I}{PI_4}\right)\\ &\quad+\frac{\gamma_Y\pi_V}{\kappa_V}(\Re_6-1)V-\frac{\gamma_Y\varkappa_V\mu_Z}{\kappa_V\sigma_Z}Z.\end{aligned}$$

Since $\Re_6 \leq 1$, then employing inequality (12), we obtain $\frac{d\Lambda_4}{dt} \leq 0$ for all $X, I, V, P, Z > 0$, Further, $\frac{d\Lambda_4}{dt} = 0$ when $X = X_4$, $I = I_4$, $P = P_4$ and $V = Z = 0$. The solutions of system (3) tend to $\tilde{\Omega}_4$ which contains elements with $P = P_4$ and $V = 0$, then $\dot{V} = \dot{P} = 0$. The fourth and fifth equations of system (3) imply

$$\begin{aligned}0 = \dot{V} = \kappa_V Y &\Longrightarrow Y(t) = 0, \text{ for all } t,\\ 0 = \dot{P} = \kappa_P I_4 - \pi_P P_4 - \varkappa_P P_4 M &\Longrightarrow M = M_4, \text{ for all } t.\end{aligned}$$

Therefore, $\tilde{\Omega}_4 = \{\Xi_4\}$, and by applying L-LAST, we obtain Ξ_4 is G.A.S.

The following result suggests that when $\Re_5 > 1$, $\Re_7 \leq 1$ and $\Re_1/\Re_2 > 1$, the IAV/SARS-CoV-2 coinfection with only stimulated SARS-CoV-2-specific antibodies is always established regardless of the initial conditions.

Theorem 6. *If* $\Re_5 > 1$, $\Re_7 \leq 1$ *and* $\Re_1/\Re_2 > 1$, *then* Ξ_5 *is G.A.S.*

Proof. Define

$$\begin{aligned}\Lambda_5 = X_5F\left(\frac{X}{X_5}\right)+Y_5F\left(\frac{Y}{Y_5}\right)+I_5F\left(\frac{I}{I_5}\right)+\frac{\gamma_Y}{\kappa_V}V_5F\left(\frac{V}{V_5}\right)\\ +\frac{\gamma_I}{\kappa_P}P_5F\left(\frac{P}{P_5}\right)+\frac{\gamma_Y\varkappa_V}{\kappa_V\sigma_Z}Z_5F\left(\frac{Z}{Z_5}\right)+\frac{\gamma_I\varkappa_P}{\kappa_P\sigma_M}M.\end{aligned}$$

□

Calculating $\frac{d\Lambda_5}{dt}$ as:

$$\begin{aligned}\frac{d\Lambda_5}{dt} &= \left(1-\frac{X_5}{X}\right)[\lambda-\alpha X-\beta_V XV-\beta_P XP]+\left(1-\frac{Y_5}{Y}\right)[\beta_V XV-\gamma_Y Y]\\ &\quad+\left(1-\frac{I_5}{I}\right)[\beta_P XP-\gamma_I I]+\frac{\gamma_Y}{\kappa_V}\left(1-\frac{V_5}{V}\right)[\kappa_V Y-\pi_V V-\varkappa_V VZ]\\ &\quad+\frac{\gamma_I}{\kappa_P}\left(1-\frac{P_5}{P}\right)[\kappa_P I-\pi_P P-\varkappa_P PM]+\frac{\gamma_Y\varkappa_V}{\kappa_V\sigma_Z}\left(1-\frac{Z_5}{Z}\right)[\sigma_Z VZ-\mu_Z Z]\\ &\quad+\frac{\gamma_I\varkappa_P}{\kappa_P\sigma_M}[\sigma_M PM-\mu_M M].\end{aligned} \tag{18}$$

Equation (18) can be simplifying as:

$$\begin{aligned}\frac{d\Lambda_5}{dt} &= \left(1-\frac{X_5}{X}\right)(\lambda-\alpha X)+\beta_V X_5 V+\beta_P X_5 P-\beta_V XV\frac{Y_5}{Y}+\gamma_Y Y_5\\ &-\beta_P XP\frac{I_5}{I}+\gamma_I I_5-\frac{\gamma_Y\pi_V}{\kappa_V}V-\gamma_Y Y\frac{V_5}{V}+\frac{\gamma_Y\pi_V}{\kappa_V}V_5+\frac{\gamma_Y\varkappa_V}{\kappa_V}V_5 Z\\ &-\frac{\gamma_I\pi_P}{\kappa_P}P-\gamma_I I\frac{P_5}{P}+\frac{\gamma_I\pi_P}{\kappa_P}P_5+\frac{\gamma_I\varkappa_P}{\kappa_P}P_5 M\\ &-\frac{\gamma_Y\varkappa_V\mu_Z}{\kappa_V\sigma_Z}Z-\frac{\gamma_Y\varkappa_V}{\kappa_V}Z_5 V+\frac{\gamma_Y\varkappa_V\mu_Z}{\kappa_V\sigma_Z}Z_5-\frac{\gamma_I\varkappa_P\mu_M}{\kappa_P\sigma_M}M.\end{aligned}$$

Using the equilibrium conditions for Ξ_5:

$$\begin{aligned}\lambda &= \alpha X_5+\beta_V X_5 V_5+\beta_P X_5 P_5,\quad \beta_V X_5 V_5=\gamma_Y Y_5,\\ \beta_P X_5 P_5 &= \gamma_I I_5,\quad Y_5=\frac{\pi_V}{\kappa_V}V_5+\frac{\varkappa_V}{\kappa_V}V_5 Z_5,\\ I_5 &= \frac{\pi_P}{\kappa_P}P_5,\quad V_5=\frac{\mu_Z}{\sigma_Z},\end{aligned}$$

we obtain,

$$\begin{aligned}\frac{d\Lambda_5}{dt} &= \left(1-\frac{X_5}{X}\right)(\alpha X_5-\alpha X)+3\beta_V X_5 V_5+3\beta_P X_5 P_5-\beta_V X_5 V_5\frac{X_5}{X}-\beta_P X_5 P_5\frac{X_5}{X}\\ &-\beta_V X_5 V_5\frac{Y_5 XV}{Y X_5 V_5}-\beta_P X_5 P_5\frac{I_5 XP}{I X_5 P_5}-\beta_V X_5 V_5\frac{V_5 Y}{V Y_5}-\beta_P X_5 P_5\frac{P_5 I}{P I_5}\\ &+\frac{\gamma_I\varkappa_P\mu_M}{\kappa_P\sigma_M}\left(\frac{\sigma_M}{\mu_M}P_5-1\right)M.\\ &= -\frac{\alpha(X-X_5)^2}{X}+\beta_V X_5 V_5\left(3-\frac{X_5}{X}-\frac{Y_5 XV}{Y X_5 V_5}-\frac{V_5 Y}{V Y_5}\right)\\ &+\beta_P X_5 P_5\left(3-\frac{X_5}{X}-\frac{I_5 XP}{I X_5 P_5}-\frac{P_5 I}{P I_5}\right)+\frac{\gamma_I\varkappa_P(\beta_P\mu_M\sigma_Z+\beta_V\mu_Z\sigma_M+\alpha\sigma_Z\sigma_M)}{\kappa_P\beta_P\sigma_M\sigma_Z}(\Re_7-1)M.\end{aligned}\tag{19}$$

Since $\Re_7\leq 1$, then employing inequality (12), we obtain $\frac{d\Lambda_5}{dt}\leq 0$ for all $X,Y,I,V,P,M>0$. Moreover, we have $\frac{d\Lambda_5}{dt}=0$ when $X=X_5$, $Y=Y_5$, $I=I_5$, $V=V_5$, $P=P_5$ and $M=0$. The trajectories of system (3) converge to $\tilde{\Omega}_5$ which comprises elements with $V=V_5$; then, $\dot{V}=0$. The fourth equation of system (3) implies that

$$0=\dot{V}=\kappa_V Y_5-\pi_V V_5-\varkappa_V V_5 Z\Longrightarrow Z(t)=Z_5,\ \text{for all } t.$$

Consequently, $\tilde{\Omega}_5=\{\Xi_5\}$, and by applying L-LAST, we obtain Ξ_5 is G.A.S.

The result given in the following theorem suggests that when $\Re_6>1$, $\Re_8\leq 1$ and $\Re_2/\Re_1>1$, the IAV/SARS-CoV-2 coinfection with only stimulated IAV-specific antibodies is always established regardless of the initial conditions.

Theorem 7. *Let* $\Re_6>1$, $\Re_8\leq 1$ *and* $\Re_2/\Re_1>1$, *then* Ξ_6 *is G.A.S.*

Proof. Consider a function Λ_6 as:

$$\begin{aligned}\Lambda_6 &= X_6 F\left(\frac{X}{X_6}\right)+Y_6 F\left(\frac{Y}{Y_6}\right)+I_6 F\left(\frac{I}{I_6}\right)+\frac{\gamma_Y}{\kappa_V}V_6 F\left(\frac{V}{V_6}\right)\\ &+\frac{\gamma_I}{\kappa_P}P_6 F\left(\frac{P}{P_6}\right)+\frac{\gamma_Y\varkappa_V}{\kappa_V\sigma_Z}Z+\frac{\gamma_I\varkappa_P}{\kappa_P\sigma_M}M_6 F\left(\frac{M}{M_6}\right).\end{aligned}$$

□

Calculating $\frac{d\Lambda_6}{dt}$ as:

$$\begin{aligned}\frac{d\Lambda_6}{dt} &= \left(1-\frac{X_6}{X}\right)[\lambda-\alpha X-\beta_V XV-\beta_P XP]+\left(1-\frac{Y_6}{Y}\right)[\beta_V XV-\gamma_Y Y]\\ &+\left(1-\frac{I_6}{I}\right)[\beta_P XP-\gamma_I I]+\frac{\gamma_Y}{\kappa_V}\left(1-\frac{V_6}{V}\right)[\kappa_V Y-\pi_V V-\varkappa_V VZ]\\ &+\frac{\gamma_I}{\kappa_P}\left(1-\frac{P_6}{P}\right)[\kappa_P I-\pi_P P-\varkappa_P PM]+\frac{\gamma_Y\varkappa_V}{\kappa_V\sigma_Z}[\sigma_Z VZ-\mu_Z Z]\\ &+\frac{\gamma_I\varkappa_P}{\kappa_P\sigma_M}\left(1-\frac{M_6}{M}\right)[\sigma_M PM-\mu_M M]. \end{aligned} \tag{20}$$

We collect the terms of Equation (20) as:

$$\begin{aligned}\frac{d\Lambda_6}{dt} &= \left(1-\frac{X_6}{X}\right)(\lambda-\alpha X)+\beta_V X_6 V+\beta_P X_6 P-\beta_V XV\frac{Y_6}{Y}+\gamma_Y Y_6-\beta_P XP\frac{I_6}{I}\\ &+\gamma_I I_6-\frac{\gamma_Y\pi_V}{\kappa_V}V-\gamma_Y Y\frac{V_6}{V}+\frac{\gamma_Y\pi_V}{\kappa_V}V_6+\frac{\gamma_Y\varkappa_V}{\kappa_V}V_6 Z-\frac{\gamma_I\pi_P}{\kappa_P}P-\gamma_I I\frac{P_6}{P}\\ &+\frac{\gamma_I\pi_P}{\kappa_P}P_6+\frac{\gamma_I\varkappa_P}{\kappa_P}P_6 M-\frac{\gamma_Y\varkappa_V\mu_Z}{\kappa_V\sigma_Z}Z-\frac{\gamma_I\varkappa_P}{\kappa_P}M_6 P+\frac{\gamma_I\varkappa_P\mu_M}{\kappa_P\sigma_M}M_6-\frac{\gamma_I\varkappa_P\mu_M}{\kappa_P\sigma_M}M.\end{aligned}$$

Using the equilibrium conditions for Ξ_6:

$$\lambda=\alpha X_6+\beta_V X_6 V_6+\beta_P X_6 P_6,\quad \beta_V X_6 V_6=\gamma_Y Y_6,\quad \beta_P X_6 P_6=\gamma_I I_6,$$
$$Y_6=\frac{\pi_V}{\kappa_V}V_6,\quad I_6=\frac{\pi_P}{\kappa_P}P_6+\frac{\varkappa_P}{\kappa_P}P_6 M_6,\quad P_6=\frac{\mu_M}{\sigma_M},$$

we obtain,

$$\begin{aligned}\frac{d\Lambda_6}{dt} &= \left(1-\frac{X_6}{X}\right)(\alpha X_6-\alpha X)+3\beta_V X_6 V_6+3\beta_P X_6 P_6-\beta_V X_6 V_6\frac{X_6}{X}-\beta_P X_6 P_6\frac{X_6}{X}\\ &-\beta_V X_6 V_6\frac{Y_6 XV}{Y X_6 V_6}-\beta_P X_6 P_6\frac{I_6 XP}{I X_6 P_6}-\beta_V X_6 V_6\frac{V_6 Y}{V Y_6}\\ &-\beta_P X_6 P_6\frac{P_6 I}{P I_6}+\frac{\gamma_Y\varkappa_V\mu_Z}{\kappa_V\sigma_Z}\left(\frac{\sigma_Z}{\mu_Z}V_6-\right)Z\\ &=-\frac{\alpha(X-X_6)^2}{X}+\beta_V X_6 V_6\left(3-\frac{X_6}{X}-\frac{Y_6 XV}{Y X_6 V_6}-\frac{V_6 Y}{V Y_6}\right)\\ &+\beta_P X_6 P_6\left(3-\frac{X_6}{X}-\frac{I_6 XP}{I X_6 P_6}-\frac{P_6 I}{P I_6}\right)\\ &+\frac{\gamma_Y\varkappa_V(\beta_P\mu_M\sigma_Z+\beta_V\mu_Z\sigma_M+\alpha\sigma_Z\sigma_M)}{\kappa_V\beta_V\sigma_M\sigma_Z}(\Re_8-1)Z.\end{aligned} \tag{21}$$

Since $\Re_8\leq 1$, then employing inequality (12), we obtain $\frac{d\Lambda_6}{dt}\leq 0$ for all $X,Y,I,V,P,Z>0$. Moreover, $\frac{d\Lambda_6}{dt}=0$ when $X=X_6$, $Y=Y_6$, $I=I_6$, $V=V_6$, $P=P_6$ and $Z=0$. The solutions of system (3) tend to $\tilde{\Omega}_6$ which contains elements with $P=P_6$; then, $\dot{P}=0$. The fifth equation of system (3) implies that

$$0=\dot{P}=\kappa_P I_6-\pi_P P_6-\varkappa_P P_6 M\Longrightarrow M(t)=M_6,\text{ for all } t.$$

Consequently, $\tilde{\Omega}_6=\{\Xi_6\}$. Using L-LAST, we deduce that Ξ_6 is G.A.S.

The following result suggests that when $\Re_7>1$ and $\Re_8>1$, the IAV/SARS-CoV-2 coinfection with both stimulated SARS-CoV-2-specific and IAV-specific antibodies is always established regardless of the initial conditions.

Theorem 8. *If* $\Re_7>1$ *and* $\Re_8>1$, *then* Ξ_7 *is G.A.S.*

Proof. Define a function Λ_7 as:

$$\Lambda_7 = X_7 F\left(\frac{X}{X_7}\right) + Y_7 F\left(\frac{Y}{Y_7}\right) + I_7 F\left(\frac{I}{I_7}\right) + \frac{\gamma_Y}{\kappa_V} V_7 F\left(\frac{V}{V_7}\right) + \frac{\gamma_I}{\kappa_P} P_7 F\left(\frac{P}{P_7}\right) + \frac{\gamma_Y \varkappa_V}{\kappa_V \sigma_Z} Z_7 F\left(\frac{Z}{Z_7}\right) + \frac{\gamma_I \varkappa_P}{\kappa_P \sigma_M} M_7 F\left(\frac{M}{M_7}\right).$$

□

Calculating $\frac{d\Lambda_7}{dt}$ as:

$$\begin{aligned}\frac{d\Lambda_7}{dt} &= \left(1 - \frac{X_7}{X}\right)[\lambda - \alpha X - \beta_V XV - \beta_P XP] + \left(1 - \frac{Y_7}{Y}\right)[\beta_V XV - \gamma_Y Y] \\ &+ \left(1 - \frac{I_7}{I}\right)[\beta_P XP - \gamma_I I] + \frac{\gamma_Y}{\kappa_V}\left(1 - \frac{V_7}{V}\right)[\kappa_V Y - \pi_V V - \varkappa_V VZ] \\ &+ \frac{\gamma_I}{\kappa_P}\left(1 - \frac{P_7}{P}\right)[\kappa_P I - \pi_P P - \varkappa_P PM] + \frac{\gamma_Y \varkappa_V}{\kappa_V \sigma_Z}\left(1 - \frac{Z_7}{Z}\right)[\sigma_Z VZ - \mu_Z Z] \\ &+ \frac{\gamma_I \varkappa_P}{\kappa_P \sigma_M}\left(1 - \frac{M_7}{M}\right)[\sigma_M PM - \mu_M M]. \end{aligned} \tag{22}$$

We collect the terms of Equation (22) as:

$$\begin{aligned}\frac{d\Lambda_7}{dt} &= \left(1 - \frac{X_7}{X}\right)(\lambda - \alpha X) + \beta_V X_7 V + \beta_P X_7 P - \beta_V XV\frac{Y_7}{Y} + \gamma_Y Y_7 \\ &- \beta_P XP\frac{I_7}{I} + \gamma_I I_7 - \frac{\gamma_Y \pi_V}{\kappa_V} V - \gamma_Y Y\frac{V_7}{V} + \frac{\gamma_Y \pi_V}{\kappa_V} V_7 + \frac{\gamma_Y \varkappa_V}{\kappa_V} V_7 Z \\ &- \frac{\gamma_I \pi_P}{\kappa_P} P - \gamma_I I\frac{P_7}{P} + \frac{\gamma_I \pi_P}{\kappa_P} P_7 + \frac{\gamma_I \varkappa_P}{\kappa_P} P_7 M - \frac{\gamma_Y \varkappa_V \mu_Z}{\kappa_V \sigma_Z} Z \\ &- \frac{\gamma_Y \varkappa_V}{\kappa_V} Z_7 V + \frac{\gamma_Y \varkappa_V \mu_Z}{\kappa_V \sigma_Z} Z_7 - \frac{\gamma_I \varkappa_P \mu_M}{\kappa_P \sigma_M} M - \frac{\gamma_I \varkappa_P}{\kappa_P} M_7 P + \frac{\gamma_I \varkappa_P \mu_M}{\kappa_P \sigma_M} M_7.\end{aligned}$$

Using the equilibrium conditions for Ξ_7:

$$\begin{aligned}&\lambda = \alpha X_7 + \beta_V X_7 V_7 + \beta_P X_7 P_7, \\ &\beta_V X_7 V_7 = \gamma_Y Y_7, \quad \beta_P X_7 P_7 = \gamma_I I_7, \\ &Y_7 = \frac{\pi_V}{\kappa_V} V_7 + \frac{\varkappa_V}{\kappa_V} V_7 Z_7, \quad I_7 = \frac{\pi_P}{\kappa_P} P_7 + \frac{\varkappa_P}{\kappa_P} P_7 M_7, \\ &V_7 = \frac{\mu_Z}{\sigma_Z}, \quad P_7 = \frac{\mu_M}{\sigma_M},\end{aligned}$$

we obtain,

$$\begin{aligned}\frac{d\Lambda_7}{dt} &= \left(1 - \frac{X_7}{X}\right)(\alpha X_7 - \alpha X) + 3\beta_V X_7 V_7 + 3\beta_P X_7 P_7 - \beta_V X_7 V_7 \frac{X_7}{X} - \beta_P X_7 P_7 \frac{X_7}{X} \\ &- \beta_V X_7 V_7 \frac{Y_7 XV}{Y X_7 V_7} - \beta_P X_7 P_7 \frac{I_7 XP}{I X_7 P_7} - \beta_V X_7 V_7 \frac{V_7 Y}{V Y_7} - \beta_P X_7 P_7 \frac{P_7 I}{P I_7} \\ &= -\frac{\alpha(X - X_7)^2}{X} + \beta_V X_7 V_7\left(3 - \frac{X_7}{X} - \frac{Y_7 XV}{Y X_7 V_7} - \frac{V_7 Y}{V Y_7}\right) \\ &+ \beta_P X_7 P_7\left(3 - \frac{X_7}{X} - \frac{I_7 XP}{I X_7 P_7} - \frac{P_7 I}{P I_7}\right).\end{aligned}$$

Using inequality (12), we obtain $\frac{d\Lambda_7}{dt} \leq 0$ for all $X, Y, I, V, P > 0$, where $\frac{d\Lambda_7}{dt} = 0$ when $X = X_7, Y = Y_7, I = I_7, V = V_7$ and $P = P_7$. The solutions of system (3) tend to $\tilde{\Omega}_7$ which

includes element with $V = V_7$ and $P = P_7$ which gives $\dot{V} = \dot{P} = 0$, and from the fourth and fifth equations of system (3), we obtain:

$$0 = \dot{V} = \kappa_V Y_7 - \pi_V V_7 - \varkappa_V V_7 Z \Longrightarrow Z(t) = Z_7, \text{ for all } t,$$
$$0 = \dot{P} = \kappa_P I_7 - \pi_P P_7 - \varkappa_P P_7 M \Longrightarrow M(t) = M_7, \text{ for all } t.$$

Therefore, $\tilde{\Omega}_7 = \{\Xi_7\}$ and by employing L-LAST, we obtain Ξ_7 is G.A.S.

Based on the above findings, we summarize the existence and global stability conditions for all equilibrium points in Table 1.

Table 1. Conditions of existence and global stability of the system's equilibria.

Equilibrium Point	Existence Conditions	Global Stability Conditions
$\Xi_0 = (X_0, 0, 0, 0, 0, 0, 0)$	None	$\Re_1 \leq 1$ and $\Re_2 \leq 1$
$\Xi_1 = (X_1, Y_1, 0, V_1, 0, 0, 0)$	$\Re_1 > 1$	$\Re_1 > 1$, $\Re_2/\Re_1 \leq 1$ and $\Re_3 \leq 1$
$\Xi_2 = (X_2, 0, I_2, 0, P_2, 0, 0)$	$\Re_2 > 1$	$\Re_2 > 1$, $\Re_1/\Re_2 \leq 1$ and $\Re_4 \leq 1$
$\Xi_3 = (X_3, Y_3, 0, V_3, 0, Z_3, 0)$	$\Re_3 > 1$	$\Re_3 > 1$ and $\Re_5 \leq 1$
$\Xi_4 = (X_4, 0, I_4, 0, P_4, 0, M_4)$	$\Re_4 > 1$	$\Re_4 > 1$ and $\Re_6 \leq 1$
$\Xi_5 = (X_5, Y_5, I_5, V_5, P_5, Z_5, 0)$	$\Re_5 > 1$ and $\Re_1/\Re_2 > 1$	$\Re_5 > 1$, $\Re_7 \leq 1$ and $\Re_1/\Re_2 > 1$
$\Xi_6 = (X_6, Y_6, I_6, V_6, P_6, 0, M_6)$	$\Re_6 > 1$ and $\Re_2/\Re_1 > 1$	$\Re_6 > 1$, $\Re_8 \leq 1$ and $\Re_2/\Re_1 > 1$
$\Xi_7 = (X_7, Y_7, I_7, V_7, P_7, Z_7, M_7)$	$\Re_7 > 1$ and $\Re_8 > 1$	$\Re_7 > 1$ and $\Re_8 > 1$

6. Numerical Simulations

The global stability of the system's equilibria will be illustrated numerically. In addition, we make a comparison between single-infection and coinfection. We use the values of the parameters presented in Table 2. Some values of parameters are taken from studies for SARS-CoV-2 single-infection and IAV single-infection, while other values are assumed just to perform the numerical simulations. To the best of our knowledge, until now there is no available data (e.g., the concentrations of SARS-CoV-2, IAV, antibodies, etc.) from SARS-CoV-2 and IAV coinfection patients. Therefore, estimating the parameters of the coinfection model is still open for future work.

Table 2. Model parameters.

Parameter	Description	Value	Source
λ	Production rate of uninfected epithelial cells	0.5	Assumed
α	Rate constant death of uninfected epithelial cells	0.05	[44,63]
γ_Y	Rate constant death of SARS-CoV-2-infected epithelial cells	0.11	[33,40,64]
γ_I	Rate constant death of IAV-infected epithelial cells	0.2	Assumed
κ_V	Rate constant of SARS-CoV-2 particles secretion per SARS-CoV-2-infected epithelial cells	0.2	[53,63]
π_V	Rate constant of SARS-CoV-2 death	0.2	[38,63]
$\varkappa_V$	Rate constant of neutralization of SARS-CoV-2 by SARS-CoV-2-specific antibodies	0.05	[38,45]
κ_P	Rate constant of IAV particles secretion per IAV-infected epithelial cells	0.4	Assumed
π_P	Rate constant of IAV death	0.1	Assumed
$\varkappa_P$	Rate constant of neutralization of IAV by IAV-specific antibodies	0.04	Assumed
μ_Z	Rate constant of natural death of SARS-CoV-2-specific antibodies	0.05	Assumed
μ_M	Rate constant of natural death of IAV-specific antibodies	0.04	[26]

6.1. Stability of the Equilibria

In this subsection, we support our global stability results provided in Theorems 1–8 by showing that the solutions of system (3) with any chosen initial conditions (any IAV/SARS-CoV-2 coinfection stage) will tend to one of the eight equilibria. Let us solve system (3) with three different initial conditions (states) as:

$$\begin{aligned}
&\text{C1}: (X(0), Y(0), I(0), V(0), P(0), Z(0), M(0)) = (8, 1, 0.5, 1, 0.5, 1, 4),\\
&\text{C2}: (X(0), Y(0), I(0), V(0), P(0), Z(0), M(0)) = (7, 1.5, 0.7, 1.5, 0.8, 2, 6),\\
&\text{C3}: (X(0), Y(0), I(0), V(0), P(0), Z(0), M(0)) = (6, 2, 1, 2, 1.4, 3, 8).
\end{aligned}$$

Selecting the values of β_V, β_P, σ_Z and σ_M leads to the following situations:

Situation 1 (Stability of Ξ_0)**:** $\beta_V = 0.001$, $\beta_P = 0.001$, $\sigma_Z = 0.01$ and $\sigma_M = 0.02$. For these values of parameters, we have $\Re_1 = 0.0909 < 1$ and $\Re_2 = 0.2 < 1$. Figure 2 shows that the trajectories tend to the equilibrium $\Xi_0 = (10, 0, 0, 0, 0, 0, 0)$ for all initials C1–C3. This demonstrates that Ξ_0 is G.A.S. based on Theorem 1. In this situation, both SARS-CoV-2 and IAV will be removed.

Situation 2 (Stability of Ξ_1)**:** $\beta_V = 0.02$, $\beta_P = 0.001$, $\sigma_Z = 0.002$ and $\sigma_M = 0.02$. With such selection, we obtain $\Re_2 = 0.2 < 1 < 1.8182 = \Re_1$, $\Re_3 = 0.1653 < 1$ and hence $\Re_2/\Re_1 = 0.11 < 1$. The equilibrium point Ξ_1 exists with $\Xi_1 = (5.5, 2.05, 0, 2.05, 0, 0, 0)$. It is clear from Figure 3 that the trajectories tend to Ξ_1 for all initials. Thus, the numerical results agree with Theorem 2. This case simulates a SARS-CoV-2 single-infection without antibody immunity. In this case, viral interference phenomenon appears, where the SARS-CoV-2 may be able to block the IAV infection.

Situation 3 (Stability of Ξ_2)**:** $\beta_V = 0.005$, $\beta_P = 0.01$, $\sigma_Z = 0.01$ and $\sigma_M = 0.005$. This gives $\Re_1 = 0.4545 < 1 < 2 = \Re_2$, $\Re_4 = 0.7692 < 1$ and then $\Re_1/\Re_2 = 0.2273 < 1$. The numerical results show that $\Xi_2 = (5, 0, 1.25, 0, 5, 0, 0)$ exists. We can observe from Figure 4 that the trajectories converge to Ξ_2 regardless of the initial states C1–C3. This result supports the result of Theorem 3. This situation represents an IAV single-infection without antibody immunity. As a result of competition between the two viruses, IAV may be able to block the SARS-CoV-2 infection.

Situation 4 (Stability of Ξ_3)**:** $\beta_V = 0.02$, $\beta_P = 0.002$, $\sigma_Z = 0.05$ and $\sigma_M = 0.05$. This yields $\Re_3 = 1.2987 > 1$ and $\Re_5 = 0.2857 < 1$. Figure 5 shows that the trajectories tend to $\Xi_3 = (7.14, 1.3, 0, 1, 0, 1.19, 0)$ regardless of the initial stats C1–C3. Therefore, Ξ_3 is G.A.S, and this supports Theorem 4. Hence, a SARS-CoV-2 single-infection with stimulated SARS-CoV-2-specific antibody is attained. Despite the activity of antibodies against the SARS-CoV-2 particles, the SARS-CoV-2 may be able to suppress the growth of IAV and block it.

Situation 5 (Stability of Ξ_4)**:** $\beta_V = 0.01$, $\beta_P = 0.05$, $\sigma_Z = 0.01$ and $\sigma_M = 0.05$. The values of $\Re_4$ and $\Re_6$ are computed as $\Re_4 = 5.5556 > 1$ and $\Re_6 = 0.5051 < 1$. Thus, Ξ_4 exists with $\Xi_4 = (5.56, 0, 1.11, 0, 0.8, 0, 11.39)$. In Figure 6, we see that the trajectories tend to Ξ_4 regardless of the initial states C1–C3. It follows that Ξ_4 is G.A.S. according to Theorem 5. Hence, an IAV single-infection with activated IAV-specific antibody is achieved. Despite the activity of antibodies against the IAV particles, the IAV may be able to block the SARS-CoV-2 infection.

Situation 6 (Stability of Ξ_5)**:** $\beta_V = 0.15$, $\beta_P = 0.04$, $\sigma_Z = 0.03$ and $\sigma_M = 0.001$. Then, we calculate $\Re_5 = 1.3333 > 1$, $\Re_7 = 0.2105 < 1$ and $\Re_1/\Re_2 = 1.7045 > 1$. The numerical results drawn in Figure 7 show that $\Xi_5 = (1.25, 2.84, 0.63, 1.67, 2.5, 2.82, 0)$ exists andis G.A.S., and this is consistent with Theorem 6. As a result, a coinfection with SARS-CoV-2 and IAV is attained where only SARS-CoV-2-specific antibody is stimulated. In this case, the concentration of the IAV particles tend to a value less than or equal to $\frac{\mu_M}{\sigma_M} = 40$, and then the IAV-specific antibody will be deactivated. On the other hand, the activity of SARS-CoV-2-specific antibodies reduces the replication of SARS-CoV-2, and this leads to the coexistence of the two viruses.

Situation 7 (Stability of Ξ_6)**:** $\beta_V = 0.04$, $\beta_P = 0.05$, $\sigma_Z = 0.01$ and $\sigma_M = 0.05$. We compute $\Re_6 = 2.0202 > 1$, $\Re_8 = 0.627 < 1$ and $\Re_2/\Re_1 = 2.75 > 1$. We find that the equilibrium $\Xi_6 = (2.75, 2.3, 0.55, 2.3, 0.8, 0, 4.38)$ exists. Further, the numerical solutions outlined in Figure 8 show that Ξ_6 is G.A.S., and this boosts the result of Theorem 7. In this situation, a coinfection with SARS-CoV-2 and IAV is attained where only the IAV-specific antibody is activated. In this case, the concentration of the SARS-CoV-2 particles tends to a value less than or equal to $\frac{\mu_Z}{\sigma_Z} = 5$, and then the SARS-CoV-2-specific antibody will be deactivated. On the other hand, the activity of IAV-specific antibodies reduces the growth of IAV, and this leads to the coexistence of the two viruses.

Situation 8 (Stability of Ξ_7)**:** $\beta_V = 0.05$, $\beta_P = 0.05$, $\sigma_Z = 0.1$ and $\sigma_M = 0.1$. This selection yields $\Re_7 = 5.2632 > 1$ and $\Re_8 = 2.3923 > 1$. Figure 9 shows that $\Xi_7 = (5.26, 1.2, 0.53, 0.5, 0.4, 5.57, 10.66)$ exists, and it is G.A.S. based on Theorem 8. In this situation, a coinfection with SARS-CoV-2 and IAV is established regardless of the initial states C1–C3. In this case, both SARS-CoV-2-specific antibody and IAV-specific antibody are working against the coinfection. The activation of both SARS-CoV-2-specific and IAV-specific antibodies leads to coexistence of the two viruses.

For more confirmation, we investigate the local stability of the system's equilibria. Calculating the Jacobian matrix $J = J(X, Y, I, V, P, Z, M)$ of system (3) as:

$$J = \begin{pmatrix} -(\alpha + \beta_V V + \beta_P P) & 0 & 0 & -\beta_V X & -\beta_P X & 0 & 0 \\ \beta_V V & -\gamma_Y & 0 & \beta_V X & 0 & 0 & 0 \\ \beta_P P & 0 & -\gamma_I & 0 & \beta_P X & 0 & 0 \\ 0 & \kappa_V & 0 & -(\pi_V + \varkappa_V Z) & 0 & -\varkappa_V V & 0 \\ 0 & 0 & \kappa_P & 0 & -(\pi_P + \varkappa_P M) & 0 & -\varkappa_P P \\ 0 & 0 & 0 & \sigma_Z Z & 0 & \sigma_Z V - \mu_Z & 0 \\ 0 & 0 & 0 & 0 & \sigma_M M & 0 & \sigma_M P - \mu_M \end{pmatrix}. \quad (23)$$

At each equilibrium, we compute the eigenvalues λ_j, $j = 1, 2, \ldots, 7$ of J. If $\mathrm{Re}(\lambda_j) < 0$, $j = 1, 2, \ldots, 7$, then the equilibrium point is locally stable. We select the parameters β_V, β_P, σ_Z and σ_M as given in situations 1–8; then, we compute all nonnegative equilibria and the accompanying eigenvalues. Table 3 outlined the nonnegative equilibria, the real parts of the eigenvalues and whether or not the equilibrium point is stable. We found that the local stability agrees with the global one.

Table 3. Local stability of nonnegative equilibria Ξ_i, $i = 0, 1, \ldots, 7$.

Situation	The Equilibria	$\mathrm{Re}(\lambda_j)$ $j = 1, 2, \ldots, 7$	Stability
1	$\Xi_0 = (10, 0, 0, 0, 0, 0, 0)$	$(-0.23, -0.22, -0.09, -0.07, -0.05, -0.05, -0.04)$	stable
2	$\Xi_0 = (10, 0, 0, 0, 0, 0, 0)$	$(-0.36, -0.23, -0.07, -0.05, -0.05, 0.05, -0.04)$	unstable
	$\Xi_1 = (5.5, 2.05, 0, 2.05, 0, 0, 0)$	$(-0.32, -0.22, -0.08, -0.04, -0.04, -0.05, -0.04)$	stable
3	$\Xi_0 = (10, 0, 0, 0, 0, 0, 0)$	$(-0.36, -0.26, 0.06, -0.05, -0.05, -0.05, -0.04)$	unstable
	$\Xi_2 = (5, 0, 1.25, 0, 5, 0, 0)$	$(-0.31, -0.24, -0.07, -0.04, -0.04, -0.05, -0.02)$	stable
4	$\Xi_0 = (10, 0, 0, 0, 0, 0, 0)$	$(-0.36, -0.25, -0.05, -0.05, 0.05, -0.05, -0.04)$	unstable
	$\Xi_1 = (5.5, 2.05, 0, 2.05, 0, 0, 0)$	$(-0.32, -0.23, -0.07, -0.04, -0.04, 0.05, -0.04)$	unstable
	$\Xi_3 = (7.14, 1.3, 0, 1, 0, 1.19, 0)$	$(-0.37, -0.24, -0.06, -0.04, -0.02, -0.02, -0.04)$	stable
5	$\Xi_0 = (10, 0, 0, 0, 0, 0, 0)$	$(-0.6, -0.3, 0.3, -0.05, -0.05, -0.04, -0.007)$	unstable
	$\Xi_2 = (1, 0, 2.25, 0, 9, 0, 0)$	$(-0.56, 0.41, -0.22, -0.12, -0.12, -0.09, -0.05)$	unstable
	$\Xi_4 = (5.56, 0, 1.11, 0, 0.8, 0, 11.39)$	$(-0.75, -0.27, -0.03, -0.03, -0.05, -0.04, -0.04)$	stable
6	$\Xi_0 = (10, 0, 0, 0, 0, 0, 0)$	$(-0.7, -0.56, 0.39, 0.25, -0.05, -0.05, -0.04)$	unstable
	$\Xi_1 = (0.73, 4.21, 0, 4.21, 0, 0, 0)$	$(-0.73, -0.27, -0.14, -0.14, 0.08, -0.04, -0.03)$	unstable
	$\Xi_2 = (1.25, 0, 2.19, 0, 8.75, 0, 0)$	$(-0.48, -0.35, -0.11, -0.11, -0.05, 0.04, -0.03)$	unstable
	$\Xi_3 = (1.67, 3.79, 0, 1.67, 0, 5.09, 0)$	$(-0.61, -0.32, -0.11, -0.11, -0.04, -0.03, 0.02)$	unstable
	$\Xi_5 = (1.25, 2.84, 0.63, 1.67, 2.5, 2.82, 0)$	$(-0.56, -0.33, -0.12, -0.12, -0.03, -0.01, -0.01)$	stable

Table 3. *Cont.*

Situation	The Equilibria	$\mathbf{Re}(\lambda_j) \quad j = 1, 2, \ldots, 7$	Stability
7	$\Xi_0 = (10, 0, 0, 0, 0, 0, 0)$	$(-0.6, -0.4, 0.3, 0.13, -0.05, -0.05, -0.04)$	unstable
	$\Xi_1 = (2.75, 3.3, 0, 3.3, 0, 0, 0)$	$(-0.39, -0.36, -0.07, -0.07, 0.09, -0.04, -0.02)$	unstable
	$\Xi_2 = (1, 0, 2.25, 0, 9, 0, 0)$	$(-0.56, 0.41, -0.26, -0.12, -0.12, -0.05, -0.05)$	unstable
	$\Xi_4 = (5.56, 0, 1.11, 0, 0.8, 0, 11.39)$	$(-0.75, -0.37, -0.03, -0.03, 0.06, -0.05, -0.04)$	unstable
	$\Xi_6 = (2.75, 2.3, 0.55, 2.3, 0.8, 0, 4.38)$	$(-0.49, -0.34, -0.06, -0.06, -0.01, -0.01, -0.03)$	stable
8	$\Xi_0 = (10, 0, 0, 0, 0, 0, 0)$	$(-0.6, -0.47, 0.3, 0.16, -0.05, -0.05, -0.04)$	unstable
	$\Xi_1 = (2.2, 3.55, 0, 3.55, 0, 0, 0)$	$(-0.38, -0.37, 0.31, -0.08, -0.08, -0.07, -0.04)$	unstable
	$\Xi_2 = (1, 0, 2.25, 0, 9, 0, 0)$	$(0.86, -0.56, -0.26, -0.12, -0.12, -0.05, -0.05)$	unstable
	$\Xi_3 = (6.67, 1.52, 0, 0.5, 0, 8.12, 0)$	$(-0.7, -0.52, 0.22, -0.02, -0.02, -0.05, -0.04)$	unstable
	$\Xi_4 = (7.14, 0, 0.71, 0, 0.4, 0, 15.36)$	$(-0.9, -0.43, 0.12, -0.02, -0.02, -0.05, -0.05)$	unstable
	$\Xi_6 = (2.2, 3.15, 0.22, 3.15, 0.4, 0, 3)$	$(-0.43, -0.36, 0.27, -0.08, -0.08, -0.006, -0.006)$	unstable
	$\Xi_7 = (5.26, 1.2, 0.53, 0.5, 0.4, 5.57, 10.66)$	$(-0.71, -0.57, -0.03, -0.03, -0.02, -0.02, -0.04)$	stable

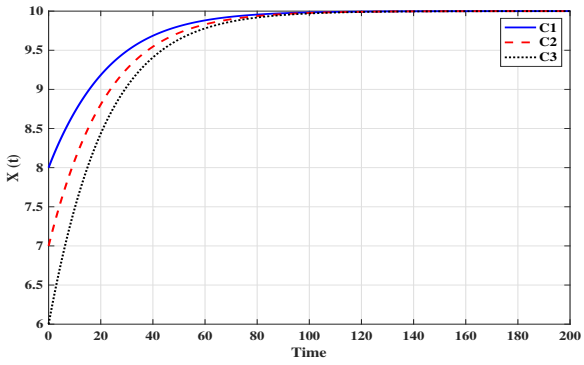

(**a**) Uninfected epithelial cells

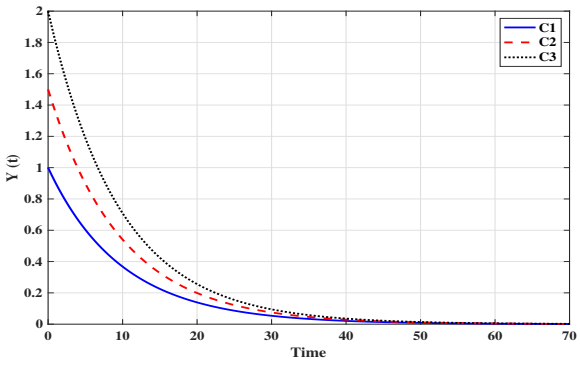

(**b**) SARS-CoV-2-infected cells

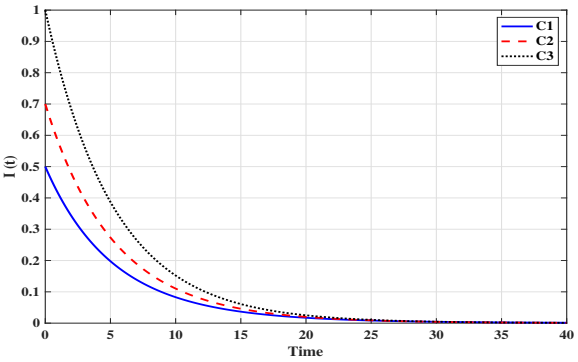

(**c**) IAV-infected cells

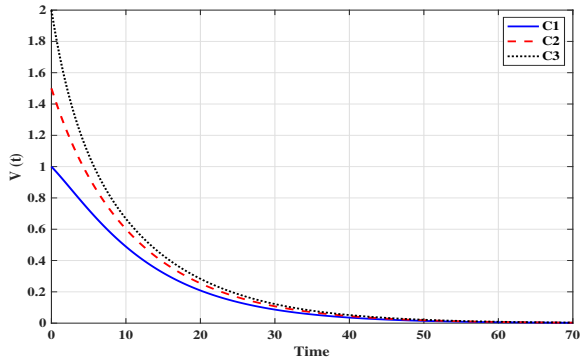

(**d**) Free SARS-CoV-2 particles

Figure 2. *Cont.*

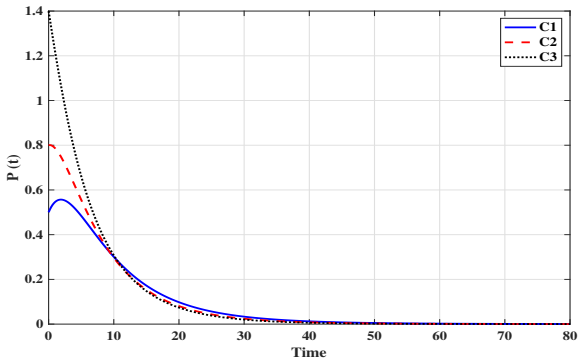

(**e**) Free IAV particles

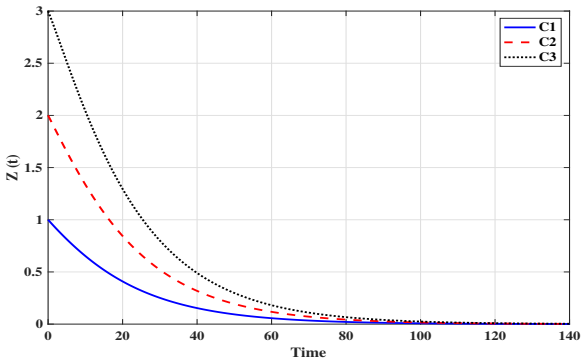

(**f**) SARS-CoV-2-specific antibodies

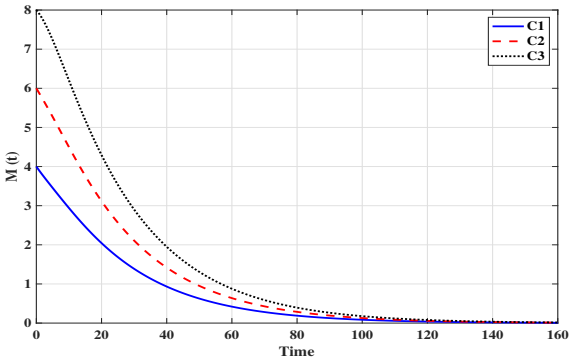

(**g**) IAV-specific antibodies

Figure 2. Solutions of system (3) with initials C1–C3 tend to $\Xi_0 = (10, 0, 0, 0, 0, 0, 0)$ when $\Re_1 \leq 1$ and $\Re_2 \leq 1$ (Situation 1).

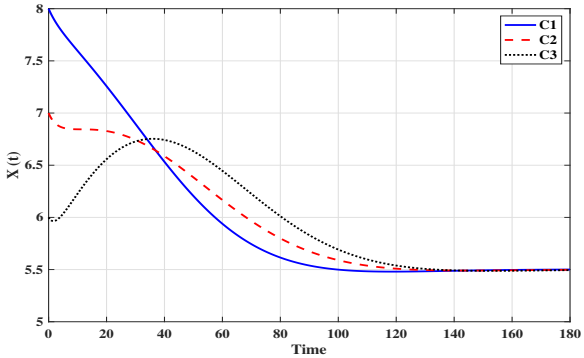

(**a**) Uninfected epithelial cells

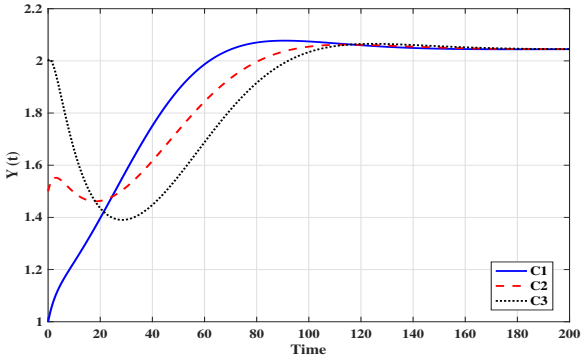

(**b**) SARS-CoV-2-infected cells

Figure 3. *Cont.*

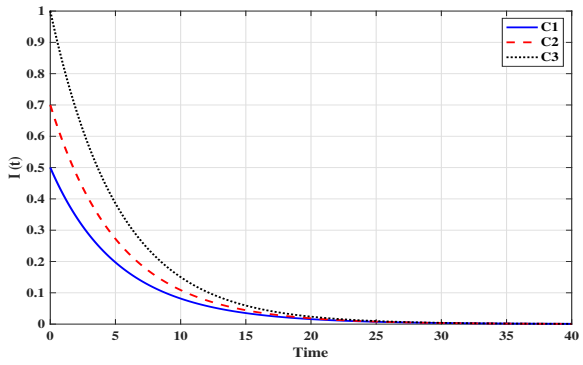

(**c**) IAV-infected cells

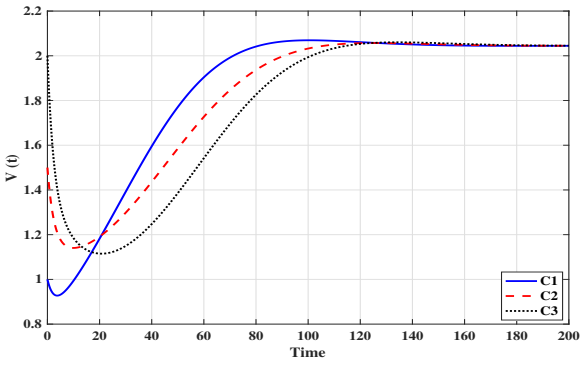

(**d**) Free SARS-CoV-2 particles

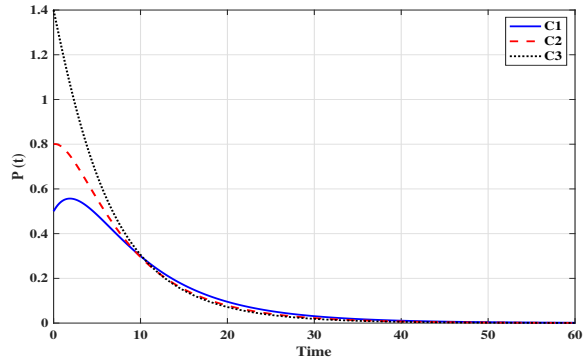

(**e**) Free IAV particles

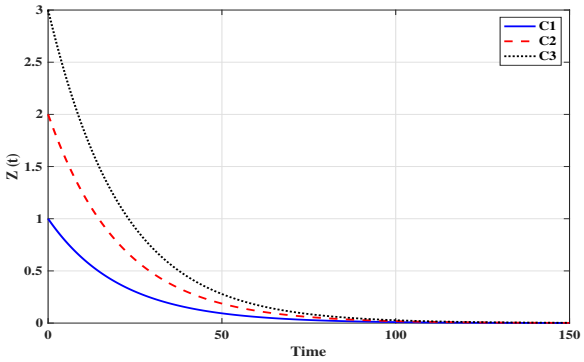

(**f**) SARS-CoV-2-specific antibodies

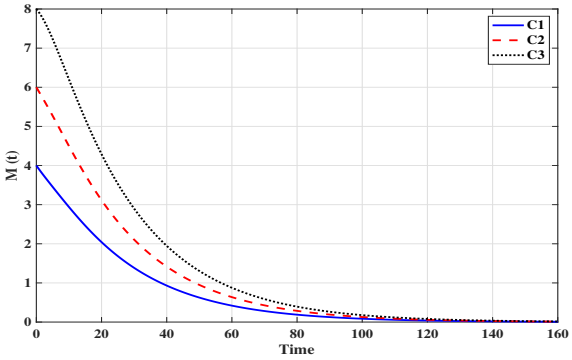

(**g**) IAV-specific antibodies

Figure 3. Solutions of system (3) with initials C1–C3 tend to $\Xi_1 = (5.5, 2.05, 0, 2.05, 0, 0, 0)$ when $\Re_1 > 1$, $\Re_2/\Re_1 \leq 1$ and $\Re_3 \leq 1$ (Situation 2).

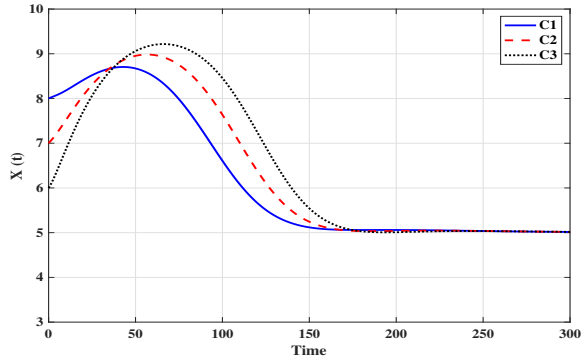

(**a**) Uninfected epithelial cells

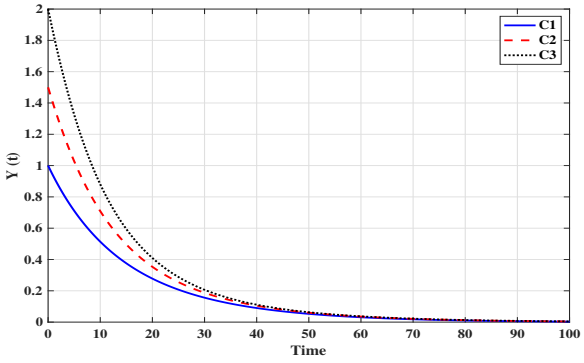

(**b**) SARS-CoV-2-infected cells

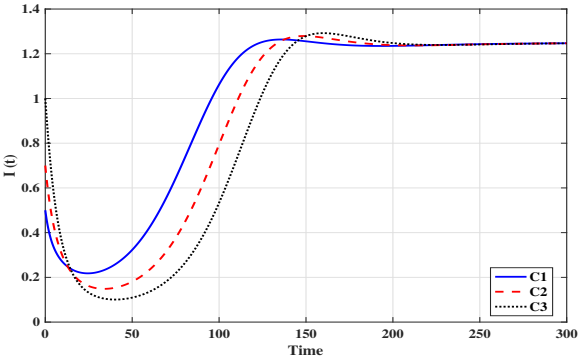

(**c**) IAV-infected cells

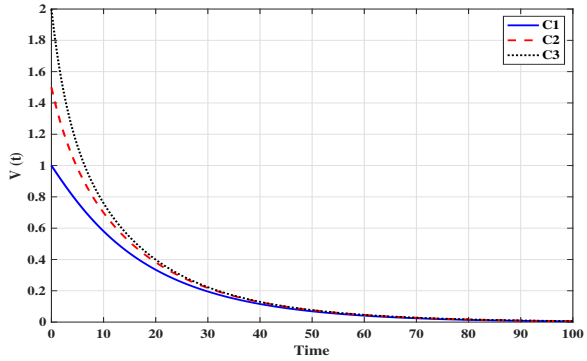

(**d**) Free SARS-CoV-2 particles

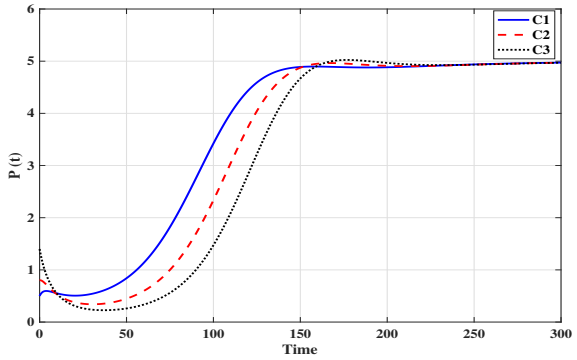

(**e**) Free IAV particles

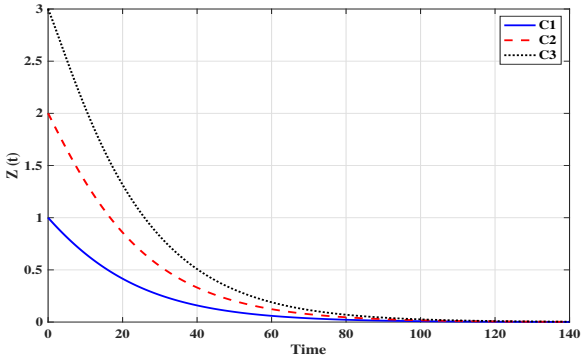

(**f**) SARS-CoV-2-specific antibodies

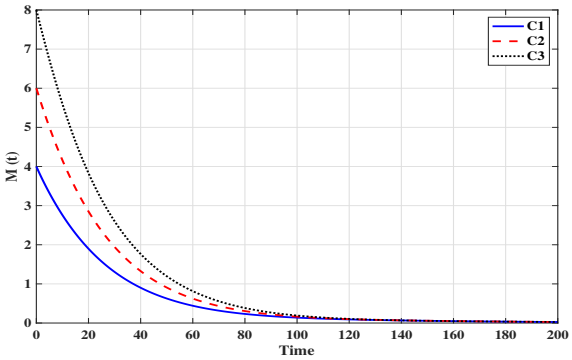

(**g**) IAV-specific antibodies

Figure 4. Solutions of system (3) with initials C1–C3 tend to $\Xi_2 = (5, 0, 1.25, 0, 5, 0, 0)$ when $\Re_2 > 1$, $\Re_1/\Re_2 \leq 1$ and $\Re_4 \leq 1$ (Situation 3).

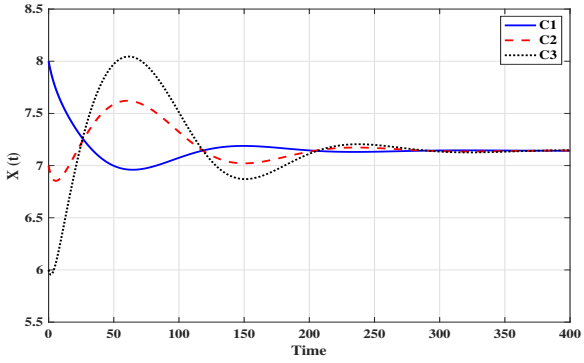

(**a**) Uninfected epithelial cells

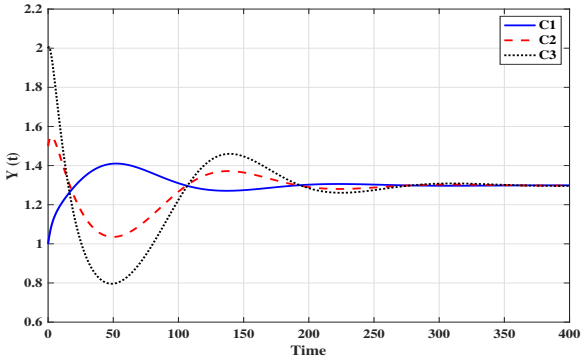

(**b**) SARS-CoV-2-infected cells

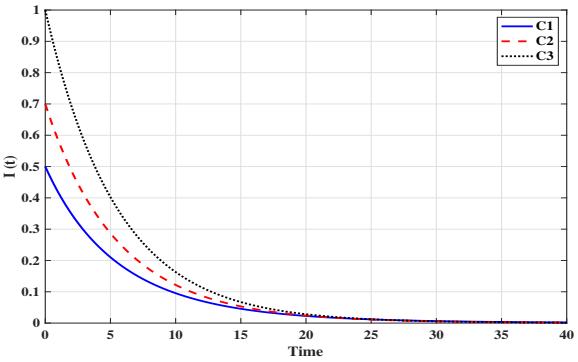

(**c**) IAV-infected cells

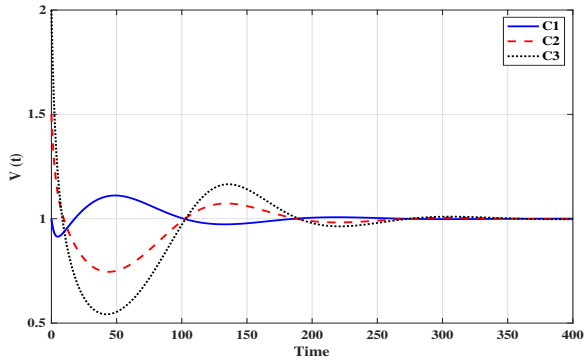

(**d**) Free SARS-CoV-2 particles

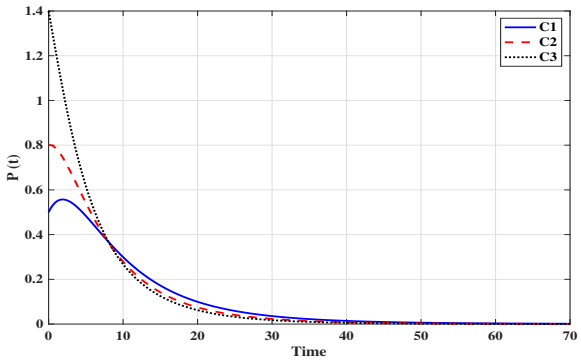

(**e**) Free IAV particles

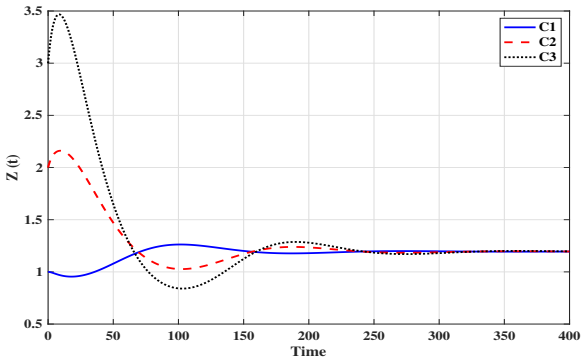

(**f**) SARS-CoV-2-specific antibodies

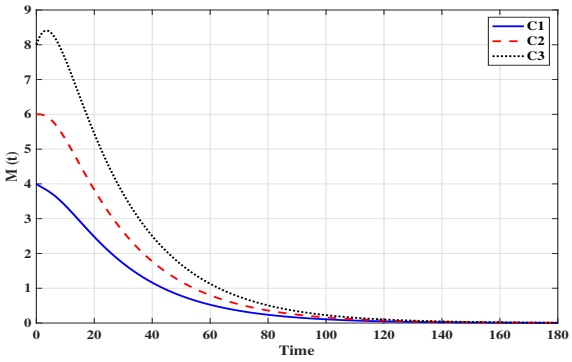

(**g**) IAV-specific antibodies

Figure 5. Solutions of system (3) with initials C1–C3 tend to $\Xi_3 = (7.14, 1.3, 0, 1, 0, 1.19, 0)$ when $\Re_3 > 1$ and $\Re_5 \leq 1$ (Situation 4).

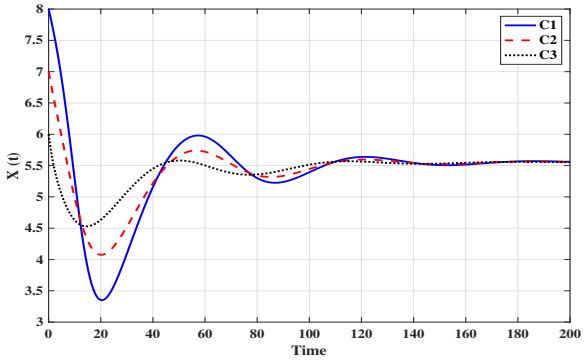

(**a**) Uninfected epithelial cells

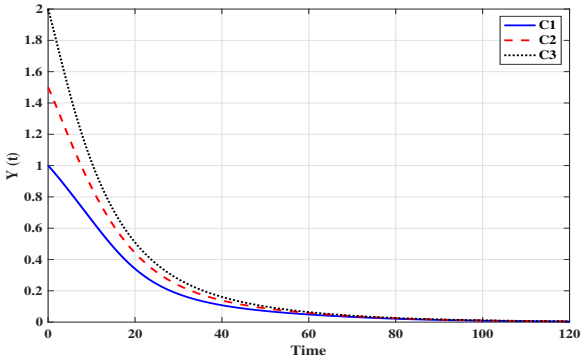

(**b**) SARS-CoV-2-infected cells

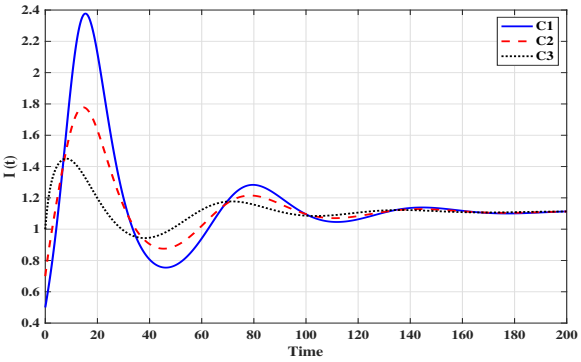

(**c**) IAV-infected cells

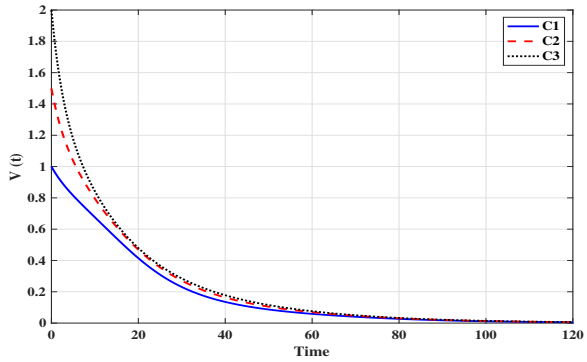

(**d**) Free SARS-CoV-2 particles

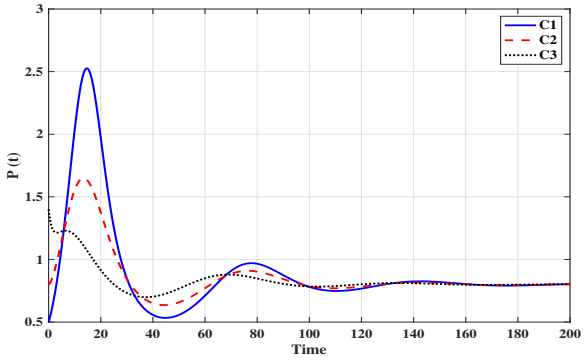

(**e**) Free IAV particles

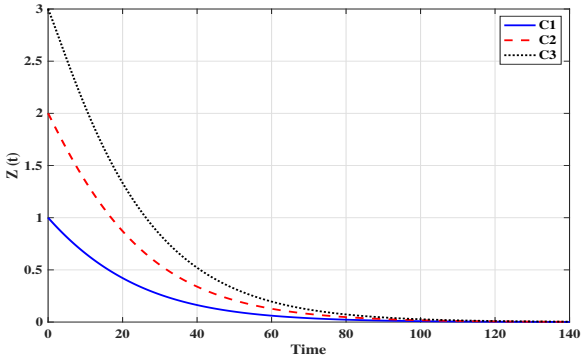

(**f**) SARS-CoV-2-specific antibodies

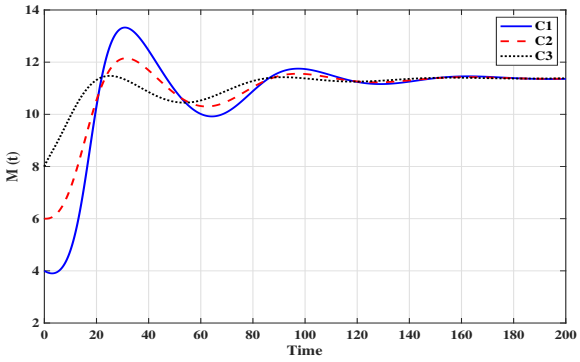

(**g**) IAV-specific antibodies

Figure 6. Solutions of system (3) with initials C1–C3 tend to $\Xi_4 = (5.56, 0, 1.11, 0, 0.8, 0, 11.39)$ when $\Re_4 > 1$ and $\Re_6 \leq 1$ (Situation 5).

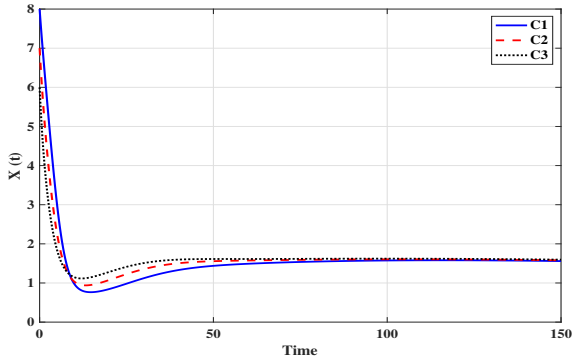

(**a**) Uninfected epithelial cells

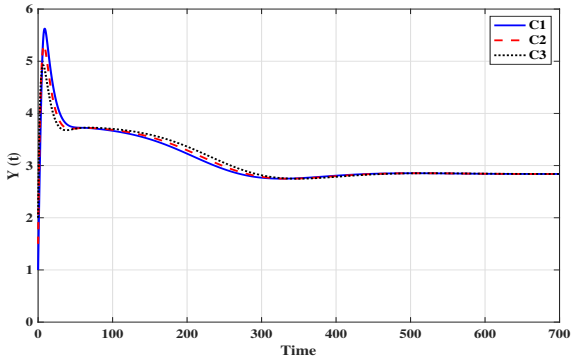

(**b**) SARS-CoV-2-infected cells

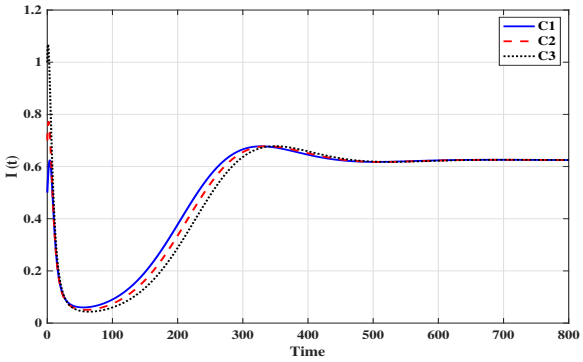

(**c**) IAV-infected cells

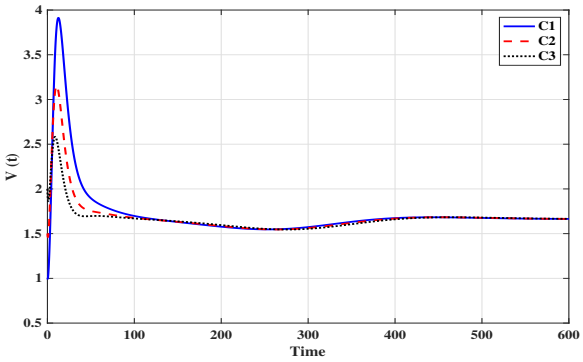

(**d**) Free SARS-CoV-2 particles

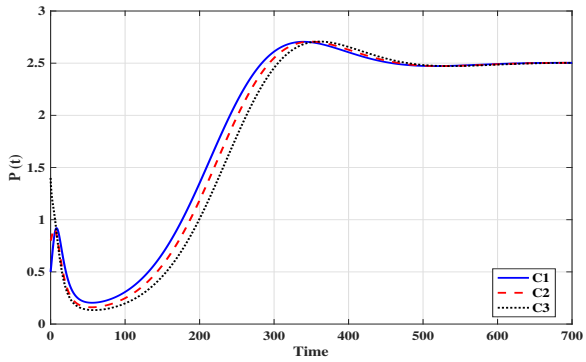

(**e**) Free IAV particles

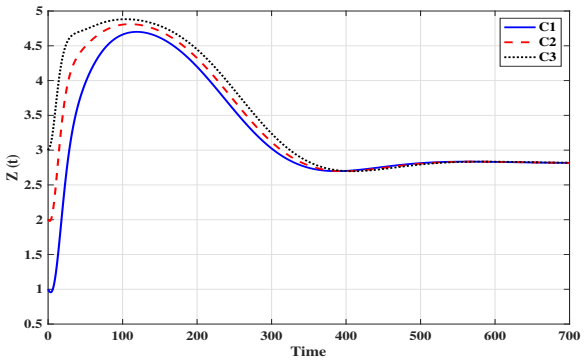

(**f**) SARS-CoV-2-specific antibodies

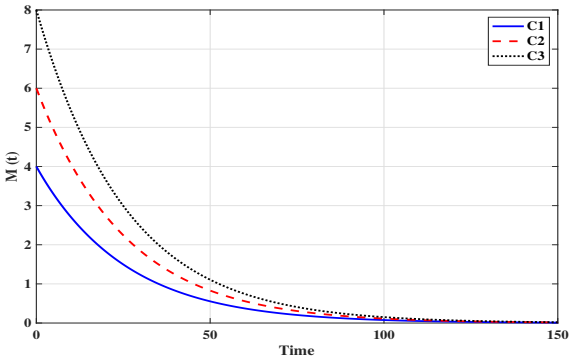

(**g**) IAV-specific antibodies

Figure 7. Solutions of system (3) with initials C1–C3 tend to $\Xi_5 = (1.25, 2.84, 0.63, 1.67, 2.5, 2.82, 0)$ when $\Re_5 > 1, \Re_1/\Re_2 > 1$ and $\Re_7 \leq 1$ (Situation 6).

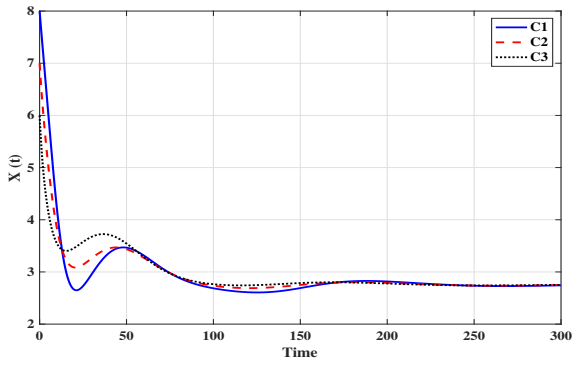

(**a**) Uninfected epithelial cells

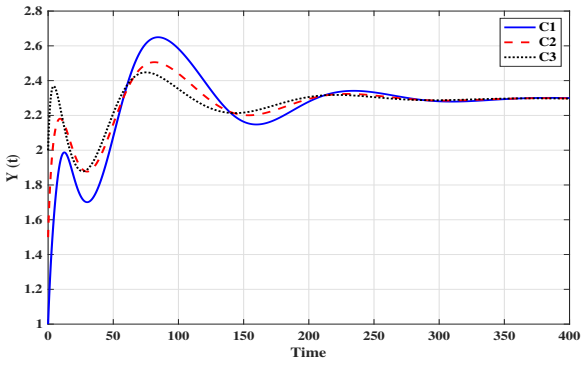

(**b**) SARS-CoV-2-infected cells

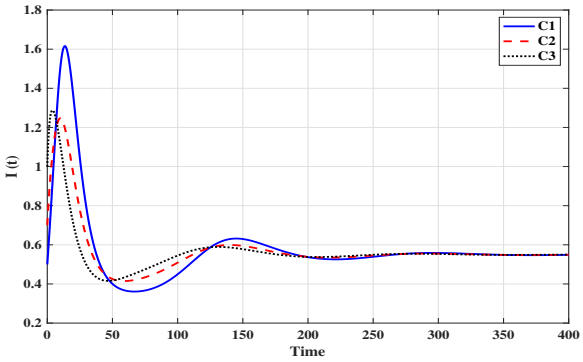

(**c**) IAV-infected cells

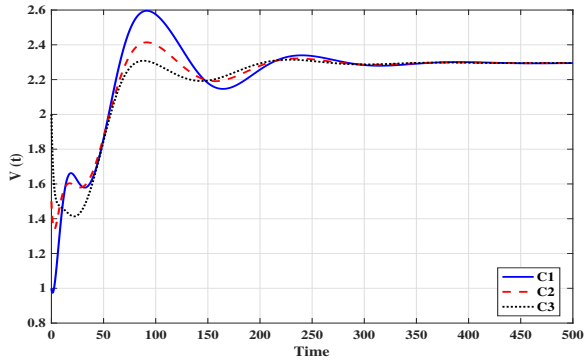

(**d**) Free SARS-CoV-2 particles

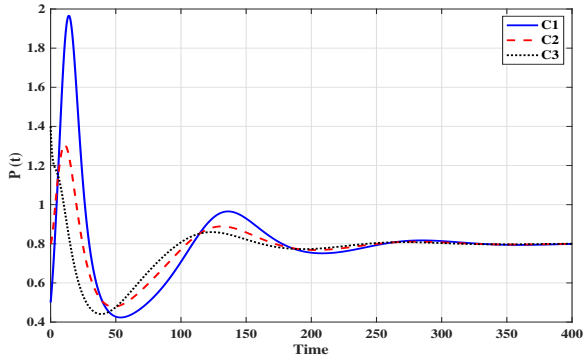

(**e**) Free IAV particles

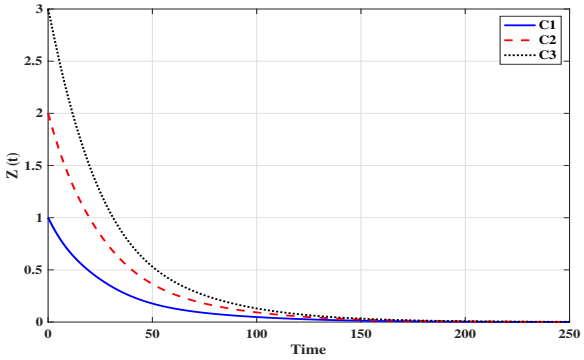

(**f**) SARS-CoV-2-specific antibodies

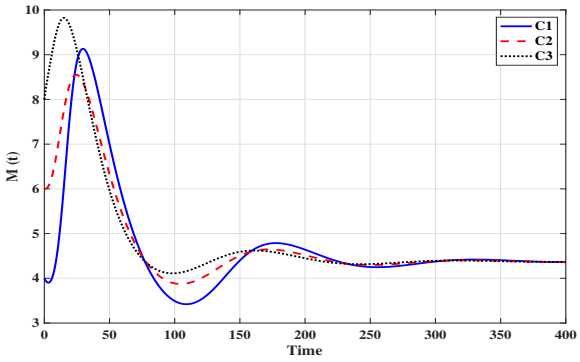

(**g**) IAV-specific antibodies

Figure 8. Solutions of system (3) with initials C1–C3 tend to $\Xi_6 = (2.75, 2.3, 0.55, 2.3, 0.8, 0, 4.38)$ when $\Re_6 > 1, \Re_2/\Re_1 > 1$ and $\Re_8 \leq 1$ (Situation 7).

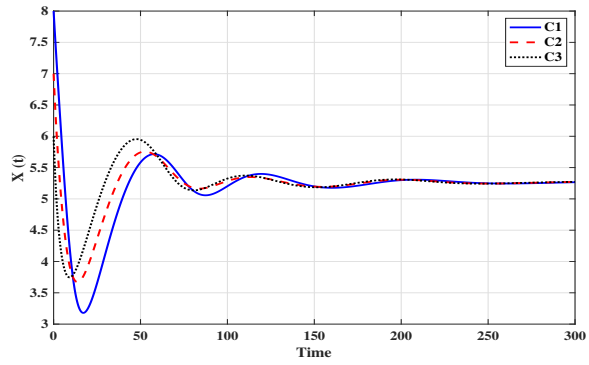

(**a**) Uninfected epithelial cells

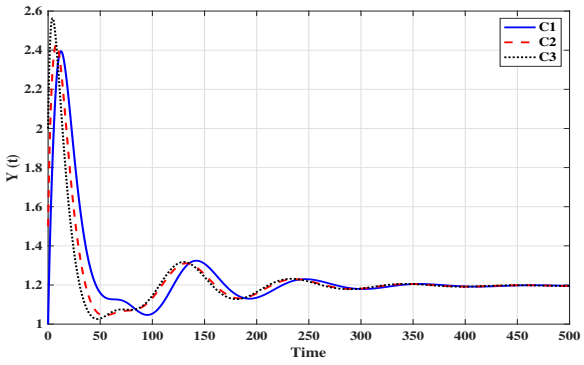

(**b**) SARS-CoV-2-infected cells

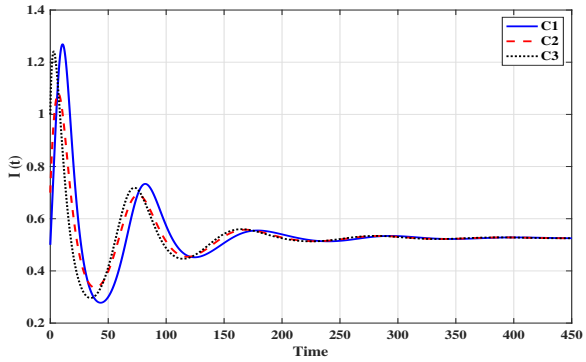

(**c**) IAV-infected cells

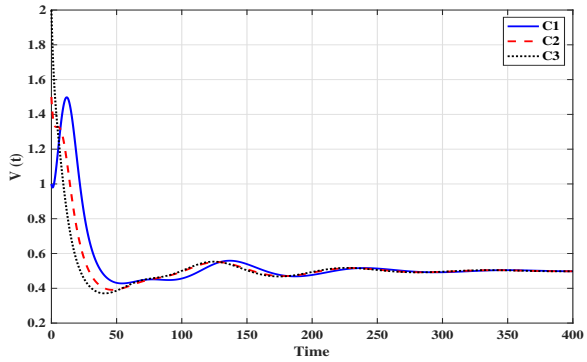

(**d**) Free SARS-CoV-2 particles

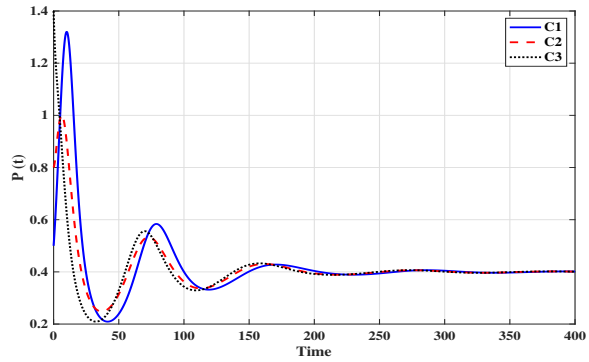

(**e**) Free IAV particles

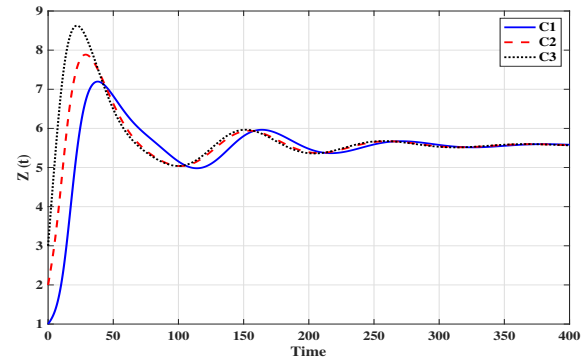

(**f**) SARS-CoV-2-specific antibodies

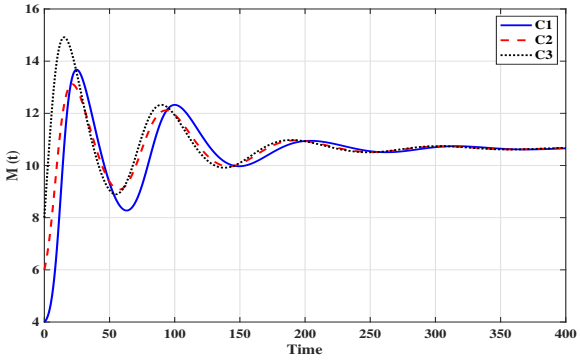

(**g**) IAV-specific antibodies

Figure 9. Solutions of system (3) with initials C1–C3 tend to $\Xi_7 = (5.26, 1.2, 0.53, 0.5, 0.4, 5.57, 10.66)$ when $\Re_7 > 1$ and $\Re_8 > 1$ (Situation 8).

6.2. Comparison Results

In this subsection, we present a comparison between the single-infection and coinfection.

Influence of IAV infection on the dynamics of SARS-CoV-2 single-infection

Here, we compare the solutions of model (3) and the following SARS-CoV-2 single-infection model:

$$\begin{cases} \dot{X} = \lambda - \alpha X - \beta_V XV, \\ \dot{Y} = \beta_V XV - \gamma_Y Y, \\ \dot{V} = \kappa_V Y - \pi_V V - \varkappa_V VZ, \\ \dot{Z} = \sigma_Z VZ - \mu_Z Z. \end{cases} \tag{24}$$

We fix parameters $\beta_V = 0.09$, $\beta_P = 0.05$, $\sigma_Z = 0.5$ and $\sigma_M = 0.9$ and select the initial state as:

$$\text{C4} : (X(0), Y(0), I(0), V(0), P(0), Z(0), M(0)) = (7.5, 0.5, 0.4, 0.03, 0.04, 7.5, 9.5)$$

From Figure 10, we observe that when the SARS-CoV-2 single-infected individual is coinfected with IAV, then the concentrations of uninfected epithelial cells, SARS-CoV-2-infected cells and SARS-CoV-2-specific antibodies are reduced. However, the concentration of free SARS-CoV-2 particles tend to be the same value in both SARS-CoV-2 single-infection and IAV/SARS-CoV-2 coinfection. This result agrees with the observation of Ding et al. [10] which said that "*IAV/SARS-CoV-2 coinfection did not result in worse clinical outcomes in comparison with SARS-CoV-2 single-infection*".

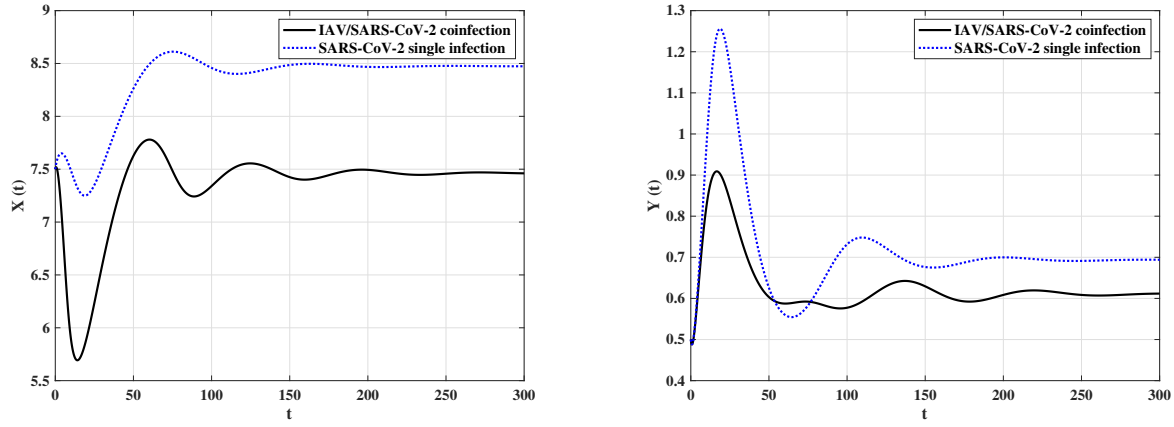

(**a**) Uninfected epithelial cells (**b**) SARS-CoV-2-infected cells

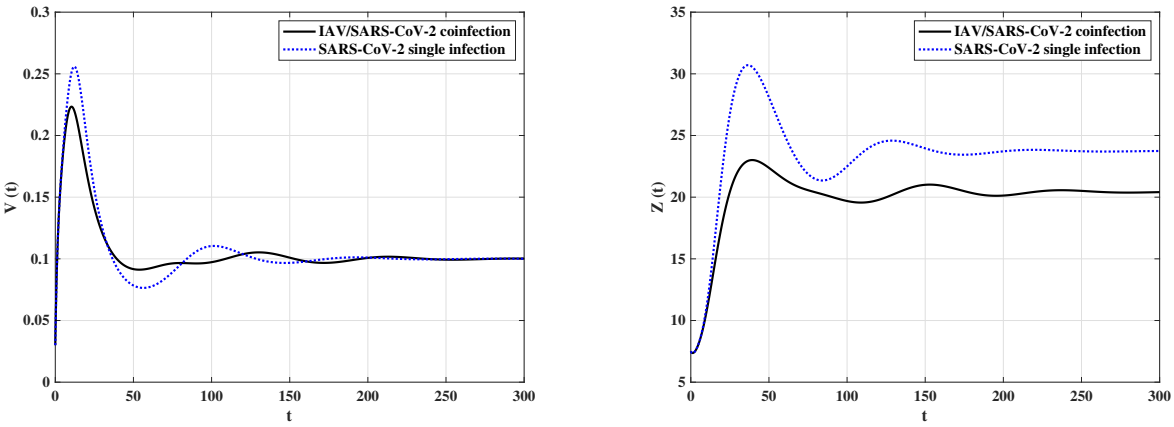

(**c**) Free SARS-CoV-2 particles (**d**) SARS-CoV-2-specific antibodies

Figure 10. Comparison between the solutions of SARS-CoV-2-single-infection model and IAV/SARS-CoV-2 coinfection model.

Influence of SARS-CoV-2 infection on the dynamics of IAV single-infection

To examine the impact of SARS-CoV-2 infection on IAV single-infection, we compare the solutions of model (3) and the following IAV single-infection model:

$$\begin{cases} \dot{X} = \lambda - \alpha X - \beta_P XP, \\ \dot{I} = \beta_P XP - \gamma_I I, \\ \dot{P} = \kappa_P I - \pi_P P - \varkappa_P PM, \\ \dot{M} = \sigma_M PM - \mu_M M. \end{cases} \tag{25}$$

We fix parameters $\beta_V = 0.095$, $\beta_P = 0.08$, $\sigma_Z = 0.9$ and $\sigma_M = 0.95$ and consider the following initial condition:

$$\text{C5} : (X(0), Y(0), I(0), V(0), P(0), Z(0), M(0)) = (6, 0.6, 0.5, 0.05, 0.05, 7.05, 8.05).$$

It can be observed from Figure 11 that when the IAV single-infected individual is coinfected with SARS-CoV-2, then the concentrations of uninfected epithelial cells, IAV-infected cells and IAV-specific antibodies are decreased. However, the concentration of free IAV particles cells tends to the same value in both IAV single-infection and IAV/SARS-CoV-2 coinfection.

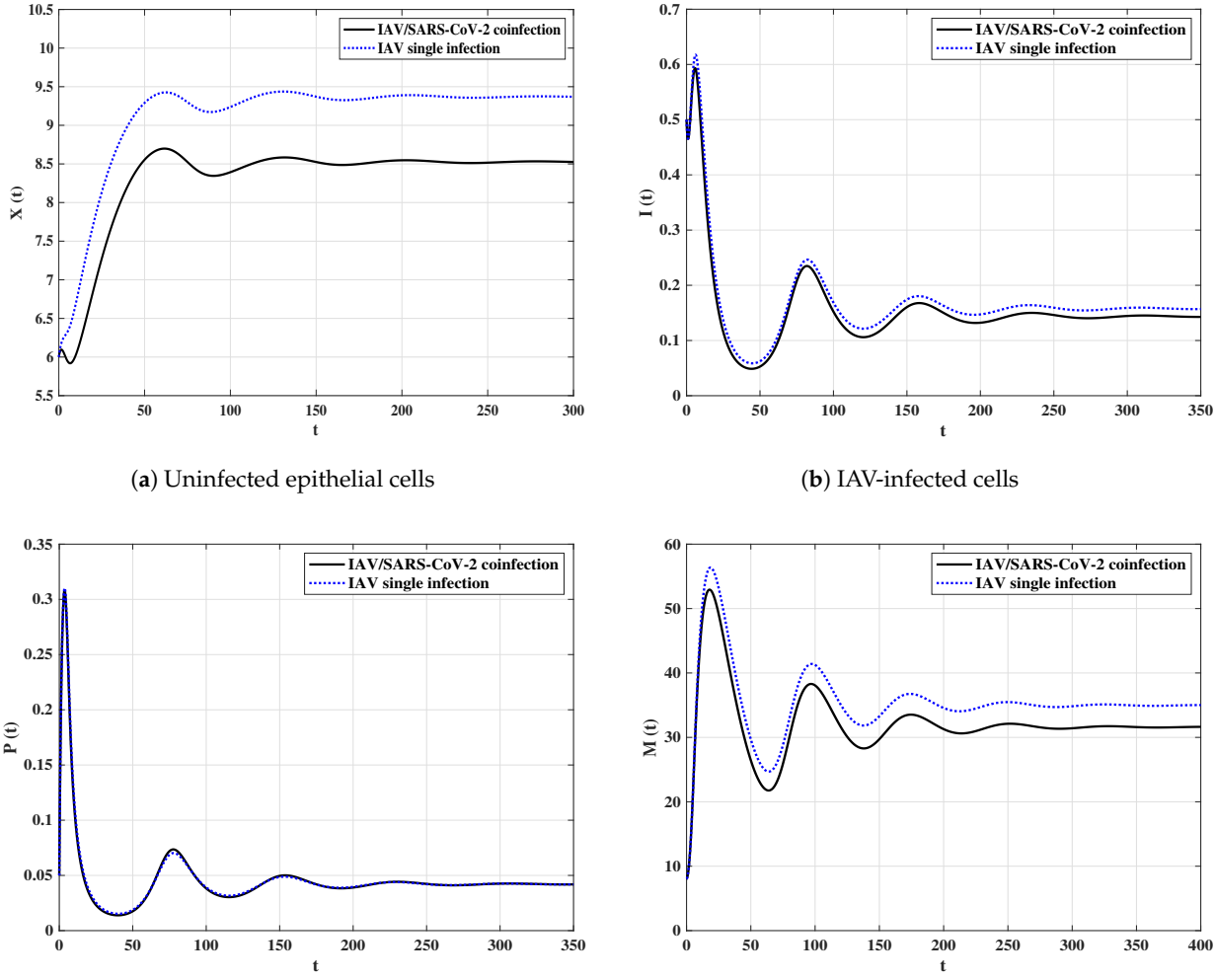

(**a**) Uninfected epithelial cells

(**b**) IAV-infected cells

(**c**) Free IAV particles

(**d**) IAV-specific antibodies

Figure 11. Comparison between the solutions of IAV-single infection model and IAV/SARS-CoV-2 coinfection model.

7. Discussion

IAV and SARS-CoV-2 coinfection cases were reported in some works (see [1,8,10,11]). Therefore, it is important to understand the within-host dynamics of this coinfection. In this paper, we develop and examine a within-host IAV/SARS-CoV-2 coinfection model. We studied the basic and global properties of the model. We find that the system has eight equilibria, and their existence and global stability are governed by eight threshold parameters ($\Re_i$, $i = 1, \ldots, 8$). We proved the following:

(I) The infection-free equilibrium Ξ_0 always exists. It is G.A.S. when $\Re_1 \leq 1$ and $\Re_2 \leq 1$. In this case, the patient is recovered from both IAV and SARS-CoV-2 infections. From a control viewpoint, making $\Re_1 \leq 1$ and $\Re_2 \leq 1$ will be a good strategy. This can be achieved by reducing the parameters β_V and β_P (or κ_V and κ_P). Let $\epsilon_V \in [0, 1]$ and $\epsilon_P \in [0, 1]$ be the effectiveness of the antiviral drugs for SARS-CoV-2 and IAV, respectively. Then, the parameters β_V and β_P will be changed to $(1 - \epsilon_V)\beta_V$ and $(1 - \epsilon_P)\beta_P$. Moreover, $\Re_1$ and $\Re_2$ become

$$\Re_1(\epsilon_V) = \frac{(1-\epsilon_V)X_0\kappa_V\beta_V}{\pi_V\gamma_Y}, \ \Re_2(\epsilon_P) = \frac{(1-\epsilon_P)X_0\kappa_P\beta_P}{\pi_P\gamma_I}.$$

To make $\Re_1 \leq 1$ and $\Re_2 \leq 1$, the effectiveness ϵ_V and ϵ_P have to satisfy

$$\epsilon_V^{\min} \leq \epsilon_V \leq 1, \ \ \epsilon_V^{\min} = \max\left\{0, 1 - \frac{1}{\Re_1(0)}\right\},$$
$$\epsilon_P^{\min} \leq \epsilon_P \leq 1, \ \ \epsilon_P^{\min} = \max\left\{0, 1 - \frac{1}{\Re_2(0)}\right\}.$$

(II) The SARS-CoV-2 single-infection equilibrium without antibody immunity Ξ_1 exists if $\Re_1 > 1$. It is G.A.S. when $\Re_1 > 1$, $\Re_2/\Re_1 \leq 1$ and $\Re_3 \leq 1$. This case leads to the situation of a patient who is only infected by SARS-CoV-2 with inactive immune response. As we will see below, if both SARS-CoV-2-specific antibody and IAV-specific antibody immunities are not activated against the two viruses, then according to the competition between the two viruses, SARS-CoV-2 may be able to block the IAV infection.

(III) The IAV single-infection equilibrium without antibody immunity Ξ_2 exists if $\Re_2 > 1$. It is G.A.S. when $\Re_2 > 1$, $\Re_1/\Re_2 \leq 1$ and $\Re_4 \leq 1$. This case leads to the situation of a patient who is only infected by IAV with unstimulated immune response. Then, IAV may be able to block the SARS-CoV-2 infection.

(IV) The SARS-CoV-2 single-infection equilibrium with stimulated SARS-CoV-2-specific antibody immunity Ξ_3 exists if $\Re_3 > 1$. It is G.A.S. when $\Re_3 > 1$ and $\Re_5 \leq 1$. This point represents the situation of a SARS-CoV-2 single-infection patient with active SARS-CoV-2-specific antibody immunity. Despite the activity of antibodies against the SARS-CoV-2 particles, the SARS-CoV-2 may be able to block the IAV.

(V) The IAV single-infection equilibrium with stimulated IAV-specific antibody immunity Ξ_4 exists if $\Re_4 > 1$. It is G.A.S. when $\Re_4 > 1$ and $\Re_6 \leq 1$. This point represents the case of an IAV single-infection patient with active IAV-specific antibody immunity. Despite the activity of antibodies against the IAV particles, the IAV may be able to block the SARS-CoV-2.

(VI) The IAV/SARS-CoV-2 coinfection equilibrium with only stimulated SARS-CoV-2-specific antibody immunity Ξ_5 exists if $\Re_5 > 1$ and $\Re_1/\Re_2 > 1$. It is G.A.S. when $\Re_5 > 1$, $\Re_7 \leq 1$ and $\Re_1/\Re_2 > 1$. Here, the IAV/SARS-CoV-2 coinfection occurs with only stimulated SARS-CoV-2-specific antibody immunity. The activity of SARS-CoV-2-specific antibodies suppresses the growth of SARS-CoV-2 particles, and this makes IAV coexist with SARS-CoV-2.

(VII) The IAV/SARS-CoV-2 coinfection equilibrium with only stimulated IAV-specific antibody immunity Ξ_6 exists if $\Re_6 > 1$ and $\Re_2/\Re_1 > 1$. It is G.A.S. when $\Re_6 > 1$, $\Re_8 \leq 1$ and $\Re_2/\Re_1 > 1$. It means that the IAV/SARS-CoV-2 coinfection occurs with only

stimulated IAV-specific antibody immunity. The activity of IAV-specific antibodies reduces the replication of IAV particles, and this makes SARS-CoV-2 coexist with IAV.

(VIII) The IAV/SARS-CoV-2 coinfection equilibrium with both stimulated SARS-CoV-2-specific antibody and IAV-specific antibody immunities Ξ_7 exists, and it is G.A.S. when $\Re_7 > 1$ and $\Re_8 > 1$. It means that the IAV/SARS-CoV-2 coinfection occurs with both SARS-CoV-2-specific antibody and IAV-specific antibody immunities activated. Since both SARS-CoV-2-specific and IAV-specific antibodies are activated, then coexistence of the two viruses appears.

We discussed the influence of IAV infection on SARS-CoV-2 single-infection dynamics and vice versa. We found that the concentration of free IAV or SARS-CoV-2 particles cells tend to be the same value in both single-infection and coinfection. This agrees with the work Ding et al. [10] which reported that IAV/SARS-CoV-2 coinfection did not result in worse clinical outcomes [10]. In addition, the spread of seasonal influenza can increase the likelihood of coinfection in patients with COVID-19 [8].

From the above, we note that the coexistence case of IAV and SARS-CoV-2 can occur if at least one type of the specific antibody immunity is active. Now, we discuss the importance of considering the antibody immune response in the IAV/SARS-CoV-2 dynamics model. If the antibody immune response is neglected, then system (3) becomes:

$$\begin{cases} \dot{X} = \lambda - \alpha X - \beta_V XV - \beta_P XP, \\ \dot{Y} = \beta_V XV - \gamma_Y Y, \\ \dot{I} = \beta_P XP - \gamma_I I, \\ \dot{V} = \kappa_V Y - \pi_V V, \\ \dot{P} = \kappa_P I - \pi_P P. \end{cases} \tag{26}$$

We can see that system (26) describes the competition between IAV and SARS-CoV-2 on one source of target cells, epithelial cells. The model admits only three equilibria:

(i) Infection-free equilibrium, $\tilde{\Xi}_0 = (\tilde{X}_0, 0, 0, 0, 0)$, where both IAV and SARS-CoV-2 are cleared,

(ii) SARS-CoV-2 single-infection equilibrium $\tilde{\Xi}_1 = (\tilde{X}_1, \tilde{Y}_1, 0, \tilde{V}_1, 0)$, where the IAV is blocked,

(iii) IAV single-infection equilibrium, $\tilde{\Xi}_2 = (\tilde{X}_2, 0, \tilde{I}_2, 0, \tilde{P}_2)$, where the SARS-CoV-2 is blocked, where $\tilde{X}_i = X_i$, $i = 0, 1, 2$, $\tilde{Y}_1 = Y_1$, $\tilde{V}_1 = V_1$, $\tilde{I}_2 = I_2$, and $\tilde{P}_2 = P_2$.

We note that the case of IAV and SARS-CoV-2 coexistence does not appear. In the recent studies presented in [1,8,10,11], it was recorded that some COVID-19 patients were coinfected with IAV. Therefore, neglecting the immune response may not describe the coinfection dynamics accurately. This supports the idea of including the immune response into the IAV/SARS-CoV-2 coinfection model, where the case of IAV and SARS-CoV-2 coexistence is observed.

8. Conclusions

Mathematical models are frequently used to understand the complex behavior of biological systems. In this paper, we formulated an IAV and SARS-CoV-2 coinfection model within a host. The model is a seven-dimensional nonlinear ODEs which describes the interaction between uninfected epithelial cells, SARS-CoV-2-infected cells, IAV-infected cells, free SARS-CoV-2 particles, free IAV particles, SARS-CoV-2-specific antibodies and IAV-specific antibodies. The regrowth and death of the uninfected epithelial cells are considered. We first examined the nonnegativity and boundedness of the solutions; then we calculated the model's equilibria and established their existence in terms of eight threshold parameters. We proved the global stability of all equilibria by constructing Lyapunov functions and applying the Lyapunov–LaSalle asymptotic stability theorem. We performed numerical simulations and demonstrated that they are in good agreement with the theoretical results. We discussed the effect of including the antibody immunity into the coinfection dynamics model. We found that including the antibody immunity in the coinfection model plays an important role in establishing the case of IAV and SARS-CoV-2 coexistence which is

practically detected in many patients. Finally, we discussed the influence of IAV infection on the dynamics of SARS-CoV-2 single-infection and vice versa.

The model proposed in this research and its analysis shows three main biological states, (i) clearance of both IAV and SARS-CoV-2 particles, (ii) appearance of interference phenomenon, where one virus may be able to suppress the growth of another virus, and (iii) coexistence of the two viruses.

The model developed in this work can be improved by (i) utilizing real data to find a good estimation of the parameters' values, (ii) studying the effect of time delays that occur during infection or production of IAV and SARS-CoV-2 particles [45], (iii) considering viral mutations [65,66], (iv) considering the effect of treatments on the progression of both viruses, and (v) including the influence of Cytotoxic T-Lymphocytes (CTLs) in killing SARS-CoV-2-infected and IAV-infected cells [40]. These research points need further investigations so we leave them to future works.

Author Contributions: Conceptualization, A.M.E. and R.S.A; Formal analysis, A.M.E, R.S.A. and A.D.H.; Investigation, A.M.E. and R.S.A; Methodology, A.M.E and A.D.H.; Writing—original draft, R.S.A.; Writing—review & editing, A.M.E. and R.S.A. All authors have read and agreed to the published version of the manuscript.

Funding: This research work was funded by Institutional Fund Projects under grant no. (IFPIP: 62-130-1443) provided by the Ministry of Education and King Abdulaziz University, DSR, Jeddah, Saudi Arabia.

Data Availability Statement: Not applicable.

Acknowledgments: This research work was funded by Institutional Fund Projects under grant no. (IFPIP: 62-130-1443). The authors gratefully acknowledge technical and financial support provided by the Ministry of Education and King Abdulaziz University, DSR, Jeddah, Saudi Arabia.

Conflicts of Interest: The authors declare no conflict of interest.

References

1. Ozaras, R. Influenza and COVID-19 coinfection: Report of six cases and review of the literature. *J. Med. Virol.* **2020**, *92*, 2657–2665. [CrossRef]
2. Coronavirus Disease (COVID-19), Weekly Epidemiological Update, World Health Organization (WHO). 2022. Available online: https://www.who.int/publications/m/item/weekly-epidemiological-update-on-covid-19---24-august-2022 (accessed on 21 August 2022).
3. Coronavirus Disease (COVID-19), Vaccine Tracker, World Health Organization (WHO). 2022. Available online: https://covid19.trackvaccines.org/agency/who/ (accessed on 2 October 2022).
4. Enomoto, T.; Shiroyama, T.; Hirata, H.; Amiya, S.; Adachi, Y.; Niitsu, T.; Noda, Y.; Hara, R.; Fukushima, K.; Suga, Y.; et al. COVID-19 in a human T-cell lymphotropic virus type-1 carrier. *Clin. Case Rep.* **2022**, *10*, e05463. [CrossRef]
5. Hernez-Vargas, E.A.; Wilk, E.; Canini, L.; Toapanta, F.R.; Binder, S.C.; Uvarovskii, A.; Meyer-Hermann, M. Effects of aging on influenza virus infection dynamics. *J. Virology* **2014**, *88*, 4123–4131. [CrossRef] [PubMed]
6. Smith, A.M.; Smith, A.P. A critical, nonlinear threshold dictates bacterial invasion and initial kinetics during influenza. *Sci. Rep.* **2016**, *6*, 38703. [CrossRef]
7. Hancioglu, B.; Swigon, D.; Clermont, G. A dynamical model of human immune response to influenza A virus infection. *J. Theor. Biol.* **2007**, *246*, 70–86. [CrossRef]
8. Zhu, X.; Ge, Y.; Wu, T.; Zhao, K.; Chen, Y.; Wu, B.; Cui, L. Co-infection with respiratory pathogens among COVID-2019 cases. *Virus Res.* **2020**, *285*, 198005. [CrossRef]
9. Aghbash, P.S.; Eslami, N.; Shirvaliloo, M.; Baghi, H. Viral coinfections in COVID-19. *J. Med Virol.* **2021**, *93*, 5310–5322. [CrossRef]
10. Ding, Q.; Lu, P.; Fan, Y.; Xia, Y.; Liu, M. The clinical characteristics of pneumonia patients coinfected with 2019 novel coronavirus and influenza virus in Wuhan, China. *J. Med Virol.* **2020**, *92*, 1549–1555. [CrossRef]
11. Wang, G.; Xie, M.; Ma, J.; Guan, J.; Song, Y.; Wen, Y.; Fang, D.; Wang, M.; Tian, D.; Li, P. Is co-Infection with Influenza Virus a Protective Factor of COVID-19? 2020. Available online: https://papers.ssrn.com/sol3/papers.cfm?abstract_id=3576904 (accessed on 2 October 2022).
12. Wang, M.; Wu, Q.; Xu, W.; Qiao, B.; Wang, J.; Zheng, H.; Li, Y. Clinical diagnosis of 8274 samples with 2019-novel coronavirus in Wuhan. *MedRxiv* **2020**. [CrossRef]
13. Lansbury, L.; Lim, B.; Baskaran, V.; Lim, W.S. Co-infections in people with COVID-19: A systematic review and meta-analysis. *J. Infect.* **2020**, *81*, 266–275. [CrossRef] [PubMed]

14. Ghaznavi, H.; Shirvaliloo, M.; Sargazi, S.; Mohammadghasemipour, Z.; Shams, Z.; Hesari, Z.; Shirvalilou, S. SARS-CoV-2 and influenza viruses: Strategies to cope with coinfection and bioinformatics perspective. *Cell Biol. Int.* **2022**, *46*, 1009–1020. [CrossRef] [PubMed]
15. Khorramdelazad, H.; Kazemi, M.H.; Najafi, A.; Keykhaee, M.; Emameh, R.Z.; Falak, R. Immunopathological similarities between COVID-19 and influenza: Investigating the consequences of co-infection. *Microb. Pathog.* **2021**, *152*, 104554. [CrossRef]
16. Xiang, X.; Wang, Z.H.; Ye, L.L.; He, X.L.; Wei, X.S.; Ma, Y.L.; Zhou, Q. Co-infection of SARS-COV-2 and influenza A virus: A case series and fast review. *Curr. Med. Sci.* **2021**, *41*, 51–57. [CrossRef] [PubMed]
17. Nowak, M.D.; Sordillo, E.M.; Gitman, M.R.; Mondolfi, A.E. Coinfection in SARS-CoV-2 infected patients: Where are influenza virus and rhinovirus/enterovirus? *J. Med. Virol.* **2020**, *92*, 1699. [CrossRef] [PubMed]
18. Pinky, L.; Dobrovolny, H.M. SARS-CoV-2 coinfections: Could influenza and the common cold be beneficial? *J. Med. Virol.* **2020**, *92*, 2623–2630. [CrossRef]
19. Pinky, L.; Dobrovolny, H.M. Coinfections of the respiratory tract: Viral competition for resources. *PLoS ONE* **2016**, *11*, e0155589. [CrossRef] [PubMed]
20. Baccam, P.; Beauchemin, C.; Macken, C.A.; Hayden, F.G.; Perelson, A. Kinetics of influenza A virus infection in humans. *J. Virol.* **2006**, *80*, 7590–7599. [CrossRef] [PubMed]
21. Smith, A.M.; Ribeiro, R.M. Modeling the viral dynamics of influenza A virus infection. *Crit. Rev. Immunol.* **2010**, *30*, 291–298. [CrossRef] [PubMed]
22. Beauchemin, C.A.; Handel, A. A review of mathematical models of influenza A infections within a host or cell culture: Lessons learned and challenges ahead. *BMC Public Health* **2011**, *11*, 1–15. [CrossRef]
23. Canini, L.; Perelson, A.S. Viral kinetic modeling: State of the art. *J. Pharmacokinet. Pharmacodyn.* **2014**, *41*, 431–443. [CrossRef]
24. Handel, A.; Liao, L.E.; Beauchemin, C.A. Progress and trends in mathematical modelling of influenza A virus infections. *Curr. Opin. Syst. Biol.* **2018**, *12*, 30–36. [CrossRef]
25. Saenz, R.A.; Quinlivan, M.; Elton, D.; MacRae, S.; Blunden, A.S.; Mumford, J.A.; Gog, J.R. Dynamics of influenza virus infection and pathology. *J. Virol.* **2010**, *84*, 3974–3983. [CrossRef] [PubMed]
26. Lee, H.Y.; Topham, D.J.; Park, S.Y.; Hollenbaugh, J.; Treanor, J.; Mosmann, T.R.; Jin, X.; Ward, B.M.; Miao, H.; Holden-Wiltse, J.; et al. Simulation and prediction of the adaptive immune response to influenza A virus infection. *J. Virol.* **2009**, *83*, 7151–7165. [CrossRef]
27. Tridane, A.; Kuang, Y. Modeling the interaction of cytotoxic T lymphocytes and influenza virus infected epithelial cells. *Math. Biosci. Eng.* **2010**, *7*, 171–185.
28. Li, K.; McCaw, J.M.; Cao, P. Modelling within-host macrophage dynamics in influenza virus infection. *J. Theor. Biol.* **2021**, *508*, 110492. [CrossRef] [PubMed]
29. Chang, D.B.; Young, C.S. Simple scaling laws for influenza A rise time, duration, and severity. *J. Theor.* **2007**, *246*, 621–635. [CrossRef]
30. Handel, A.; Longini, I.M., Jr.; Antia, R. Towards a quantitative understanding of the within-host dynamics of influenza A infections. *J. R. Soc. Interface* **2010**, *7*, 35–47. [CrossRef] [PubMed]
31. Handel, A.; Longini, I.M., Jr.; Antia, R. Neuraminidase inhibitor resistance in influenza: Assessing the danger of its generation and spread. *PLoS Comput. Biol.* **2007**, *3*, e240. [CrossRef] [PubMed]
32. Hernandez-Vargas, E.A.; Velasco-Hernandez, J.X. In-host mathematical modelling of COVID-19 in humans. *Annu. Rev. Control* **2020**, *50*, 448–456. [CrossRef]
33. Li, C.; Xu, J.; Liu, J.; Zhou, Y. The within-host viral kinetics of SARS-CoV-2. *Math. Biosci. Eng.* **2020**, *17*, 2853–2861. [CrossRef] [PubMed]
34. Ke, R.; Zitzmann, C.; Ho, D.D.; Ribeiro, R.M.; Perelson, A.S. In vivo kinetics of SARS-CoV-2 infection and its relationship with a person's infectiousness. *Proc. Natl. Acad. Sci. USA* **2021**, *118*, e2111477118. [CrossRef] [PubMed]
35. Gonçalves, A.; Bertrand, J.; Ke, R.; Comets, E.; de Lamballerie, X.; Malvy, D.; Pizzorno, A.; Terrier, O.; Calatrava, M.R.; Mentré, F. Timing of antiviral treatment initiation is critical to reduce SARS-CoV-2 viral load. *CPT Pharmacomet. Syst. Pharmacol.* **2020**, *9*, 509–514. [CrossRef] [PubMed]
36. Wang, S.; Pan, Y.; Wang, Q.; Miao, H.; Brown, A.N.; Rong, L. Modeling the viral dynamics of SARS-CoV-2 infection. *Math. Biosci.* **2020**, *328*, 108438. [CrossRef] [PubMed]
37. Sadria, M.; Layton, A.T. Modeling within-host SARS-CoV-2 infection dynamics and potential treatments. *Viruses* **2021**, *13*, 1141. [CrossRef] [PubMed]
38. Ghosh, I. Within host dynamics of SARS-CoV-2 in humans: modeling immune responses and antiviral treatments. *SN Comput. Sci.* **2021**, *2*, 482. [CrossRef]
39. Du, S.Q.; Yuan, W. Mathematical modeling of interaction between innate and adaptive immune responses in COVID-19 and implications for viral pathogenesis. *J. Med Virol.* **2020**, *92*, 1615–1628. [CrossRef] [PubMed]
40. Hattaf, K.; Yousfi, N. Dynamics of SARS-CoV-2 infection model with two modes of transmission and immune response. *Math. Biosci. Eng.* **2020**, *17*, 5326–5340. [CrossRef] [PubMed]
41. Almoceraa, A.E.S.; Quiroz, G.; Hernandez-Vargas, E.A. Stability analysis in COVID-19 within-host model with immune response. *Commun. Nonlinear Sci. Numer.* **2021**, *95*, 105584. [CrossRef]

42. Mondal, J.; Samui, P.; Chatterjee, A.N. Dynamical demeanour of SARS-CoV-2 virus undergoing immune response mechanism in COVID-19 pandemic. *Eur. Phys. J. Spec. Top.* **2022**. [CrossRef]
43. Abuin, P.; Anderson, A.; Ferramosca, A.; Hernandez-Vargas, E.A.; Gonzalez, A.H. Characterization of SARS-CoV-2 dynamics in the host. *Annu. Rev. Control* **2020**, *50*, 457–468. [CrossRef]
44. Chhetri, B.; Bhagat, V.M.; Vamsi, D.K.K.; Ananth, V.S.; Prakash, D.B.; Mandale, R.; Muthusamy, S.; Sanjeevi, C.B. Within-host mathematical modeling on crucial inflammatory mediators and drug interventions in COVID-19 identifies combination therapy to be most effective and optimal. *Alex. Eng. J.* **2021**, *60*, 2491–2512. [CrossRef]
45. Elaiw, A.M.; Alsaedi, A.J.; Agha, A.D.A.; Hobiny, A.D. Global stability of a humoral immunity COVID-19 model with logistic growth and delays. *Mathematics* **2022**, *10*, 1857. [CrossRef]
46. Ringa, N.; Diagne, M.L.; Rwezaura, H.; Omame, A.; Tchuenche, S.Y.T.J.M. HIV and COVID-19 co-infection: A mathematical model and optimal control. *Inform. Med. Unlocked* **2022**, *31*, 100978. [CrossRef]
47. Rehman, A.; Singh, R.; Agarwal, P. Modeling, analysis and prediction of new variants of covid-19 and dengue co-infection on complex network. *Chaos Solitons Fractals* **2021**, *150*, 111008. [CrossRef]
48. Omame, A.; Abbas, M.; Abdel-Aty, A. Assessing the impact of SARS-CoV-2 infection on the dynamics of dengue and HIV via fractional derivatives. *Chaos Solitons Fractals* **2022**, *162*, 112427. [CrossRef]
49. Omame, A.; Abbas, M.; Onyenegecha, C.P. Backward bifurcation and optimal control in a co-infection model for, SARS-CoV-2 and ZIKV. *Results Phys.* **2022**, *37*, 105481. [CrossRef]
50. Pérez, A.G.; Oluyori, D.A. A model for COVID-19 and bacterial pneumonia coinfection with community-and hospital-acquired infections. *arXiv* **2022**, arXiv:2207.13265.
51. Ojo, M.M.; Benson, T.O.; Peter, O.J.; Goufo, E.F.D. Nonlinear optimal control strategies for a mathematical model of COVID-19 and influenza co-infection. *Phys. A Stat. Mech. Its Appl.* **2022**, *607*, 128173. [CrossRef]
52. Mekonen, K.G.; Obsu, L.L. Mathematical modeling and analysis for the co-infection of COVID-19 and tuberculosis. *Heliyon* **2022**, *8*, e11195. [CrossRef]
53. Agha, A.D.A.; Elaiw, A.M.; Ramadan, S.A.A.E. Stability analysis of within-host SARS-CoV-2/HIV coinfection model. *Math. Methods Appl. Sci.* **2022**, 1–20. [CrossRef]
54. Agha, A.D.A.; Elaiw, A.M. Global dynamics of SARS-CoV-2/malaria model with antibody immune response. *Math. Eng.* **2022**, *19*, 8380–8410. [CrossRef]
55. Zhou, Y.; Huang, M.; Jiang, Y.A.; Zou, X. Data-driven mathematical modeling and dynamical analysis for SARS-CoV-2 coinfection with bacteria. *Int. J. Bifurc. Chaos* **2021**, *31*, 2150163. [CrossRef]
56. Barik, M.; Swarup, C.; Singh, T.; Habbi, S.; Chauhan, S. Dynamical analysis, optimal control and spatial pattern in an influenza model with adaptive immunity in two stratified population. *AIMS Math.* **2021**, *7*, 4898–4935. [CrossRef]
57. Danchin, A.; Pagani-Azizi, O.; Turinici, G.; Yahiaoui, G. COVID-19 adaptive humoral immunity models: Non-neutralizing versus antibody-disease enhancement scenarios. *medRxiv* **2020**. [CrossRef]
58. Korobeinikov, A. Global properties of basic virus dynamics models. *Bull. Math. Biol.* **2004**, *66*, 879–883. [CrossRef]
59. Barbashin, E.A. *Introduction to the Theory of Stability*; Wolters-Noordhoff: Groningen, The Netherlands, 1970.
60. LaSalle, J.P. *The Stability of Dynamical Systems*; SIAM: Philadelphia, PA, USA, 1976.
61. Lyapunov, A.M. *The General Problem of the Stability of Motion*; Taylor & Francis, Ltd.: London, UK, 1992.
62. Hale, J.K.; Lunel, S.V. *Introduction to Functional Differential Equations*; Springer: New York, NY, USA, 1993.
63. Odaka, M.; Inoue, K. Modeling viral dynamics in SARS-CoV-2 infection based on differential equations and numerical analysis. *Heliyon* **2021**, *7*, e08207. [CrossRef]
64. Nath, B.J.; Dehingia, K.; Mishra, V.N.; Chu, Y.-M.; Sarmah, H.K. Mathematical analysis of a within-host model of SARS-CoV-2. *Adv. Differ. Equations* **2021**, *2021*, 113. [CrossRef]
65. Bellomo, N.; Burini, D.; Outada, N. Multiscale models of Covid-19 with mutations and variants. *Netw. Heterog. Media.* **2022**, *17*, 293–310. [CrossRef]
66. Bellomo, N.; Burini, D.; Outada, N. Pandemics of mutating virus and society: A multi-scale active particles approach. *Philos. Trans. A Math. Phys. Eng. Sci.* **2022**, *380*, 1–14. [CrossRef]